

Order-Independent Constraint-Based Causal Structure Learning

Diego Colombo

Marloes H. Maathuis

Seminar for Statistics

ETH Zurich

8092 Zurich, Switzerland

COLOMBO@STAT.MATH.ETHZ.CH

MAATHUIS@STAT.MATH.ETHZ.CH

Editor: Peter Spirtes

Abstract

We consider constraint-based methods for causal structure learning, such as the PC-, FCI-, RFCI- and CCD- algorithms (Spirtes et al., 1993, 2000; Richardson, 1996; Colombo et al., 2012; Claassen et al., 2013). The first step of all these algorithms consists of the adjacency search of the PC-algorithm. The PC-algorithm is known to be order-dependent, in the sense that the output can depend on the order in which the variables are given. This order-dependence is a minor issue in low-dimensional settings. We show, however, that it can be very pronounced in high-dimensional settings, where it can lead to highly variable results. We propose several modifications of the PC-algorithm (and hence also of the other algorithms) that remove part or all of this order-dependence. All proposed modifications are consistent in high-dimensional settings under the same conditions as their original counterparts. We compare the PC-, FCI-, and RFCI-algorithms and their modifications in simulation studies and on a yeast gene expression data set. We show that our modifications yield similar performance in low-dimensional settings and improved performance in high-dimensional settings. All software is implemented in the R-package `pcaIlg`.

Keywords: directed acyclic graph, PC-algorithm, FCI-algorithm, CCD-algorithm, order-dependence, consistency, high-dimensional data

1. Introduction

Constraint-based methods for causal structure learning use conditional independence tests to obtain information about the underlying causal structure. We start by discussing several prominent examples of such algorithms, designed for different settings.

The PC-algorithm (Spirtes et al., 1993, 2000) was designed for learning directed *acyclic* graphs (DAGs) under the assumption of *causal sufficiency*, i.e., no unmeasured common causes and no selection variables. It learns a Markov equivalence class of DAGs that can be uniquely described by a so-called completed partially directed acyclic graph (CPDAG) (see Section 2 for a precise definition). The PC-algorithm is widely used in high-dimensional settings (Kalisch et al., 2010; Nagarajan et al., 2010; Stekhoven et al., 2012; Zhang et al., 2012), since it is computationally feasible for sparse graphs with up to thousands of variables, and open-source software is available, for example in TETRAD IV (Spirtes et al., 2000) and the R-package `pcaIlg` (Kalisch et al., 2012). Moreover, the PC-algorithm has been shown

to be consistent for high-dimensional sparse graphs (Kalisch and Bühlmann, 2007; Harris and Drton, 2013).

The FCI- and RFCI-algorithms and their modifications (Spirtes et al., 1993, 2000, 1999; Spirtes, 2001; Zhang, 2008; Colombo et al., 2012; Claassen et al., 2013) were designed for learning directed *acyclic* graphs when *allowing for latent and selection variables*. Thus, these algorithms learn a Markov equivalence class of DAGs with latent and selection variables, which can be uniquely represented by a partial ancestral graph (PAG). These algorithms first employ the adjacency search of the PC-algorithm, and then perform additional conditional independence tests because of the latent variables.

Finally, the CCD-algorithm (Richardson, 1996) was designed for learning Markov equivalence classes of directed (*not necessarily acyclic*) graphs under the assumption of *causal sufficiency*. Again, the first step of this algorithm consists of the adjacency search of the PC-algorithm.

Hence, all these algorithms share the adjacency search of the PC-algorithm as a common first step. We will therefore focus our analysis on this algorithm, since any improvements to the PC-algorithm can be directly carried over to the other algorithms. When the PC-algorithm is applied to data, it is generally order-dependent, in the sense that its output depends on the order in which the variables are given. Dash and Druzdzel (1999) exploit the order-dependence to obtain candidate graphs for a score-based approach. Cano et al. (2008) resolve the order-dependence via a rather involved method based on measuring edge strengths. Spirtes et al. (2000) (Section 5.4.2.4) propose a method that removes the “weakest” edges as early as possible. Overall, however, the order-dependence of the PC-algorithm has received relatively little attention in the literature, suggesting that it seems to be regarded as a minor issue. We found, however, that the order-dependence can become very problematic for high-dimensional data, leading to highly variable results and conclusions for different variable orderings.

In particular, we analyzed the yeast gene expression data set of Hughes et al. (2000). We chose these data, despite the existence of larger and newer yeast gene expression data sets, since these data contain both observational and experimental data, obtained under similar conditions. The observational data consist of gene expression levels of 5361 genes for 63 wild-type yeast organisms, and the experimental data consist of gene expression levels of the same 5361 genes for 234 single-gene knockout strains. Hence, these data form a nice test bed for causal inference: algorithms can be applied to the observational data, and their output can be compared to the “gold standard” experimental data. (Please see Section 6 for more detailed information about the data.)

First, we considered estimating the skeleton of the CPDAG from the observational data, that is, the undirected graph obtained by discarding all arrowheads in the CPDAG. Figure 1(a) shows the large variability in the estimated skeletons for 25 random orderings of the variables. Each estimated skeleton consists of roughly 5000 edges which can be divided into three groups: about 1500 are highly stable and occur in all orderings, about 1500 are moderately stable and occur in at least 50% of the orderings, and about 2000 are unstable and occur in at most 50% of the orderings. Since the FCI- and CCD-algorithms employ the adjacency search of the PC-algorithm as a first step, their resulting skeletons for these data are also highly order-dependent.

An important motivation for learning DAGs lies in their causal interpretation. We therefore also investigated the effect of different variable orderings on causal inference that is based on the PC-algorithm. In particular, we applied the IDA algorithm (Maathuis et al., 2010, 2009) to the observational yeast gene expression data, for 25 random variable orderings. The IDA algorithm conceptually consists of two-steps: one first estimates the Markov equivalence class of DAGs using the PC-algorithm, and one then applies Pearl’s do-calculus (Pearl, 2000) to each DAG in the Markov equivalence class. (The algorithm uses a fast local implementation that does not require listing all DAGs in the equivalence class.) One can then obtain estimated lower bounds on the sizes of the causal effects between all pairs of genes. For each of the 25 random variable orderings, we ranked the gene pairs according to these lower bounds, and compared these rankings to a gold standard set of large causal effects computed from the experimental single gene knock-out data, as in Maathuis et al. (2010). Figure 1(b) shows the large variability in the resulting receiver operating characteristic (ROC) curves. The ROC curve that was published in Maathuis et al. (2010) was significantly better than random guessing with $p < 0.001$, and is somewhere in the middle. Some of the other curves are much better, while there are also curves that are indistinguishable from random guessing.

The remainder of the paper is organized as follows. In Section 2 we discuss some background and terminology. Section 3 explains the original PC-algorithm. Section 4 introduces modifications of the PC-algorithm (and hence also of the (R)FCI- and CCD-algorithms) that remove part or all of the order-dependence. These modifications are identical to their original counterparts when perfect conditional independence information is used. When applied to data, the modified algorithms are partly or fully order-independent. Moreover, they are consistent in high-dimensional settings under the same conditions as the original algorithms. Section 5 compares all algorithms in simulations, and Section 6 compares them on the yeast gene expression data discussed above. We close with a discussion in Section 7.

2. Preliminaries

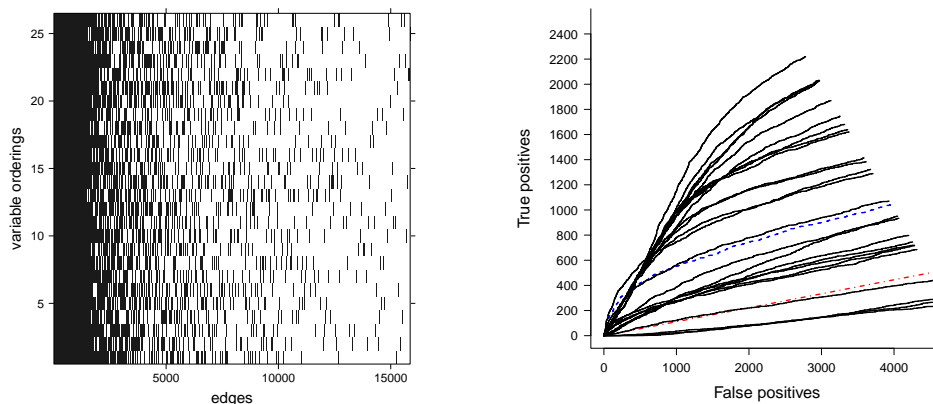
In this section, we introduce some necessary terminology and background information.

2.1 Graph Terminology

A graph $\mathcal{G} = (\mathbf{V}, \mathbf{E})$ consists of a vertex set $\mathbf{V} = \{X_1, \dots, X_p\}$ and an edge set \mathbf{E} . The vertices represent random variables and the edges represent relationships between pairs of variables.

A graph containing only directed edges (\rightarrow) is *directed*, one containing only undirected edges ($-$) is *undirected*, and one containing directed and/or undirected edges is *partially directed*. The *skeleton* of a partially directed graph is the undirected graph that results when all directed edges are replaced by undirected edges.

All graphs we consider are *simple*, meaning that there is at most one edge between any pair of vertices. If an edge is present, the vertices are said to be *adjacent*. If all pairs of vertices in a graph are adjacent, the graph is called *complete*. The *adjacency set* of a vertex X_i in a graph $\mathcal{G} = (\mathbf{V}, \mathbf{E})$, denoted by $\text{adj}(\mathcal{G}, X_i)$, is the set of all vertices in \mathbf{V} that are adjacent to X_i in \mathcal{G} . A vertex X_j in $\text{adj}(\mathcal{G}, X_i)$ is called a *parent* of X_i if $X_j \rightarrow X_i$. The corresponding set of parents is denoted by $\text{pa}(\mathcal{G}, X_i)$.



(a) Edges occurring in the estimated skeletons for 25 random variable orderings, as well as for the original ordering (shown as variable ordering 26). A black entry for an edge i and a variable ordering j means that edge i occurred in the estimated skeleton for the j th variable ordering. The edges along the x -axis are ordered according to their frequency of occurrence in the estimated skeletons, from edges that occurred always to edges that occurred only once. Edges that did not occur for any of the variable orderings were omitted. For technical reasons, only every 10th edge is actually plotted.

(b) ROC curves corresponding to the 25 random orderings of the variables (solid black), where the curves are generated exactly as in Maathuis et al. (2010). The ROC curve for the original ordering of the variables (dashed blue) was published in Maathuis et al. (2010). The dashed-dotted red curve represents random guessing.

Figure 1: Analysis of the yeast gene expression data (Hughes et al., 2000) for 25 random orderings of the variables, using tuning parameter $\alpha = 0.01$. The estimated graphs and resulting causal rankings are highly order-dependent.

A *path* is a sequence of distinct adjacent vertices. A *directed path* is a path along directed edges that follows the direction of the arrowheads. A *directed cycle* is formed by a directed path from X_i to X_j together with the edge $X_j \rightarrow X_i$. A (partially) directed graph is called a (*partially*) *directed acyclic graph* if it does not contain directed cycles.

A triple (X_i, X_j, X_k) in a graph \mathcal{G} is *unshielded* if X_i and X_j as well as X_j and X_k are adjacent, but X_i and X_k are not adjacent in \mathcal{G} . A *v-structure* (X_i, X_j, X_k) is an unshielded triple in a graph \mathcal{G} where the edges are oriented as $X_i \rightarrow X_j \leftarrow X_k$.

2.2 Probabilistic and Causal Interpretation of DAGs

We use the notation $X_i \perp\!\!\!\perp X_j | \mathbf{S}$ to indicate that X_i is independent of X_j given \mathbf{S} , where \mathbf{S} is a set of variables not containing X_i and X_j (Dawid, 1980). If \mathbf{S} is the empty set, we simply write $X_i \perp\!\!\!\perp X_j$. If $X_i \perp\!\!\!\perp X_j | \mathbf{S}$, we refer to \mathbf{S} as a *separating set* for (X_i, X_j) . A

separating set \mathbf{S} for (X_i, X_j) is called *minimal* if there is no proper subset \mathbf{S}' of \mathbf{S} such that $X_i \perp\!\!\!\perp X_j | \mathbf{S}'$.

A distribution Q is said to *factorize* according to a DAG $\mathcal{G} = (\mathbf{V}, \mathbf{E})$ if the joint density of $\mathbf{V} = (X_1, \dots, X_p)$ can be written as the product of the conditional densities of each variable given its parents in \mathcal{G} : $q(X_1, \dots, X_p) = \prod_{i=1}^p q(X_i | \text{pa}(\mathcal{G}, X_i))$.

A DAG entails conditional independence relationships via a graphical criterion called *d-separation* (Pearl, 2000). If two vertices X_i and X_j are not adjacent in a DAG \mathcal{G} , then they are d-separated in \mathcal{G} by a subset \mathbf{S} of the remaining vertices. If X_i and X_j are d-separated by \mathbf{S} , then $X_i \perp\!\!\!\perp X_j | \mathbf{S}$ in any distribution Q that factorizes according to \mathcal{G} . A distribution Q is said to be *faithful* to a DAG \mathcal{G} if the reverse implication also holds, that is, if the conditional independence relationships in Q are exactly the same as those that can be inferred from \mathcal{G} using d-separation.

Several DAGs can describe exactly the same conditional independence information. Such DAGs are called Markov equivalent and form a Markov equivalence class. Markov equivalent DAGs have the same skeleton and the same v-structures, and a Markov equivalence class can be described uniquely by a completed partially directed acyclic graph (CPDAG) (Andersson et al., 1997; Chickering, 2002). A CPDAG is a partially directed acyclic graph with the following properties: every directed edge exists in every DAG in the Markov equivalence class, and for every undirected edge $X_i - X_j$ there exists a DAG with $X_i \rightarrow X_j$ and a DAG with $X_i \leftarrow X_j$ in the Markov equivalence class. A CPDAG \mathcal{C} is said to *represent* a DAG \mathcal{G} if \mathcal{G} belongs to the Markov equivalence class described by \mathcal{C} .

A DAG can be interpreted causally in the following way (Pearl, 2000, 2009; Spirtes et al., 2000): X_1 is a direct cause of X_2 only if $X_1 \rightarrow X_2$, and X_1 is a possibly indirect cause of X_2 only if there is a directed path from X_1 to X_2 .

3. The PC-Algorithm

We now describe the PC-algorithm in detail. In Section 3.1, we discuss the algorithm under the assumption that we have perfect conditional independence information between all variables in \mathbf{V} . We refer to this as the *oracle version*. In Section 3.2 we discuss the more realistic situation where conditional independence relationships have to be estimated from data. We refer to this as the *sample version*.

3.1 Oracle Version

A sketch of the PC-algorithm is given in Algorithm 3.1. We see that the algorithm consists of three steps. Step 1 (also called *adjacency search*) finds the skeleton and separation sets, while Steps 2 and 3 determine the orientations of the edges.

Step 1 is given in pseudo-code in Algorithm 3.2. We start with a complete undirected graph \mathcal{C} . This graph is subsequently thinned out in the loop on lines 3-15 in Algorithm 3.2, where an edge $X_i - X_j$ is deleted if $X_i \perp\!\!\!\perp X_j | \mathbf{S}$ for some subset \mathbf{S} of the remaining variables. These conditional independence queries are organized in a way that makes the algorithm computationally efficient for high-dimensional sparse graphs, since we only need to query conditional independencies up to order $q - 1$, where q is the maximum size of the adjacency sets of the nodes in the underlying DAG.

Algorithm 3.1 The PC-algorithm (oracle version)

Require: Conditional independence information among all variables in \mathbf{V} , and an ordering $\text{order}(\mathbf{V})$ on the variables

- 1: Adjacency search: Find the skeleton \mathcal{C} and separation sets using Algorithm 3.2;
 - 2: Orient unshielded triples in the skeleton \mathcal{C} based on the separation sets;
 - 3: In \mathcal{C} orient as many of the remaining undirected edges as possible by repeated application of rules R1-R3 (see text);
 - 4: **return** Output graph (\mathcal{C}) and separation sets (sepset).
-

Algorithm 3.2 Adjacency search / Step 1 of the PC-algorithm (oracle version)

Require: Conditional independence information among all variables in \mathbf{V} , and an ordering $\text{order}(\mathbf{V})$ on the variables

- 1: Form the complete undirected graph \mathcal{C} on the vertex set \mathbf{V}
 - 2: Let $\ell = -1$;
 - 3: **repeat**
 - 4: Let $\ell = \ell + 1$;
 - 5: **repeat**
 - 6: Select a (new) ordered pair of vertices (X_i, X_j) that are adjacent in \mathcal{C} and satisfy $|\text{adj}(\mathcal{C}, X_i) \setminus \{X_j\}| \geq \ell$, using $\text{order}(\mathbf{V})$;
 - 7: **repeat**
 - 8: Choose a (new) set $\mathbf{S} \subseteq \text{adj}(\mathcal{C}, X_i) \setminus \{X_j\}$ with $|\mathbf{S}| = \ell$, using $\text{order}(\mathbf{V})$;
 - 9: **if** X_i and X_j are conditionally independent given \mathbf{S} **then**
 - 10: Delete edge $X_i - X_j$ from \mathcal{C} ;
 - 11: Let $\text{sepset}(X_i, X_j) = \text{sepset}(X_j, X_i) = \mathbf{S}$;
 - 12: **end if**
 - 13: **until** X_i and X_j are no longer adjacent in \mathcal{C} or all $\mathbf{S} \subseteq \text{adj}(\mathcal{C}, X_i) \setminus \{X_j\}$ with $|\mathbf{S}| = \ell$ have been considered
 - 14: **until** all ordered pairs of adjacent vertices (X_i, X_j) in \mathcal{C} with $|\text{adj}(\mathcal{C}, X_i) \setminus \{X_j\}| \geq \ell$ have been considered
 - 15: **until** all pairs of adjacent vertices (X_i, X_j) in \mathcal{C} satisfy $|\text{adj}(\mathcal{C}, X_i) \setminus \{X_j\}| \leq \ell$
 - 16: **return** \mathcal{C} , sepset.
-

First, when $\ell = 0$, all pairs of vertices are tested for marginal independence. If $X_i \perp\!\!\!\perp X_j$, then the edge $X_i - X_j$ is deleted and the empty set is saved as separation set in $\text{sepset}(X_i, X_j)$ and $\text{sepset}(X_j, X_i)$. After all pairs of vertices have been considered (and many edges might have been deleted), the algorithm proceeds to the next step with $\ell = 1$.

When $\ell = 1$, the algorithm chooses an ordered pair of vertices (X_i, X_j) still adjacent in \mathcal{C} , and checks $X_i \perp\!\!\!\perp X_j | \mathbf{S}$ for subsets \mathbf{S} of size $\ell = 1$ of $\text{adj}(\mathcal{C}, X_i) \setminus \{X_j\}$. If such a conditional independence is found, the edge $X_i - X_j$ is removed, and the corresponding conditioning set \mathbf{S} is saved in $\text{sepset}(X_i, X_j)$ and $\text{sepset}(X_j, X_i)$. If all ordered pairs of adjacent vertices have been considered for conditional independence given all subsets of size ℓ of their adjacency sets, the algorithm again increases ℓ by one. This process continues until all adjacency sets in the current graph are smaller than ℓ . At this point the skeleton and the separation sets have been determined.

We see that this procedure indeed ensures that we only query conditional independencies up to order $q - 1$, where q is the maximum size of the adjacency sets of the nodes in the underlying DAG. This makes the algorithm particularly efficient for large sparse graphs.

Step 2 determines the v-structures. In particular, it considers all unshielded triples in \mathcal{C} , and orients an unshielded triple (X_i, X_j, X_k) as a v-structure if and only if $X_j \notin \text{sepset}(X_i, X_k)$.

Finally, Step 3 orients as many of the remaining undirected edges as possible by repeated application of the following three rules:

- R1: orient $X_j - X_k$ into $X_j \rightarrow X_k$ whenever there is a directed edge $X_i \rightarrow X_j$ such that X_i and X_k are not adjacent (otherwise a new v-structure is created);
- R2: orient $X_i - X_j$ into $X_i \rightarrow X_j$ whenever there is a chain $X_i \rightarrow X_k \rightarrow X_j$ (otherwise a directed cycle is created);
- R3: orient $X_i - X_j$ into $X_i \rightarrow X_j$ whenever there are two chains $X_i - X_k \rightarrow X_j$ and $X_i - X_l \rightarrow X_j$ such that X_k and X_l are not adjacent (otherwise a new v-structure or a directed cycle is created).

The PC-algorithm was shown to be sound and complete.

Theorem 1 (*Theorem 5.1 on p.410 of Spirtes et al., 2000*) *Let the distribution of \mathbf{V} be faithful to a DAG $\mathcal{G} = (\mathbf{V}, \mathbf{E})$, and assume that we are given perfect conditional independence information about all pairs of variables (X_i, X_j) in \mathbf{V} given subsets $\mathbf{S} \subseteq \mathbf{V} \setminus \{X_i, X_j\}$. Then the output of the PC-algorithm is the CPDAG that represents \mathcal{G} .*

We briefly discuss the main ingredients of the proof, as these will be useful for understanding our modifications in Section 4. The faithfulness assumption implies that conditional independence in the distribution of \mathbf{V} is equivalent to d-separation in the graph \mathcal{G} . The skeleton of \mathcal{G} can then be determined as follows: X_i and X_j are adjacent in \mathcal{G} if and only if they are conditionally dependent given any subset \mathbf{S} of the remaining nodes. Naively, one could therefore check all these conditional dependencies, which is known as the SGS-algorithm (Spirtes et al., 2000). The PC-algorithm obtains the same result with fewer tests, by using the following fact about DAGs: two variables X_i and X_j in a DAG \mathcal{G} are d-separated by some subset \mathbf{S} of the remaining variables if and only if they are d-separated

by $\text{pa}(\mathcal{G}, X_i)$ or $\text{pa}(\mathcal{G}, X_j)$. The PC-algorithm is guaranteed to check these conditional independencies: at all stages of the algorithm, the graph \mathcal{C} is a supergraph of the true CPDAG, and the algorithm checks conditional dependencies given all subsets of the adjacency sets, which obviously include the parent sets.

The v-structures are determined based on Lemmas 5.1.2 and 5.1.3 of Spirtes et al. (2000). The soundness and completeness of the orientation rules in Step 3 was shown in Meek (1995) and Andersson et al. (1997).

3.2 Sample Version

In applications, we of course do not have perfect conditional independence information. Instead, we assume that we have an i.i.d. sample of size n of $\mathbf{V} = (X_1, \dots, X_p)$. A sample version of the PC-algorithm can then be obtained by replacing all conditional independence queries by statistical conditional independence tests at some pre-specified significance level α . For example, if the distribution of \mathbf{V} is multivariate Gaussian, one can test for zero partial correlation, see, e.g., Kalisch and Bühlmann (2007). This is the test we used throughout this paper.

We note that the PC-algorithm performs many tests. Hence, α should not be interpreted as an overall significance level. Rather, it plays the role of a tuning parameter, where smaller values of α tend to lead to sparser graphs.

3.3 Order-Dependence in the Sample Version

Let $\text{order}(\mathbf{V})$ denote an ordering on the variables in \mathbf{V} . We now consider the role of $\text{order}(\mathbf{V})$ in every step of the algorithm. Throughout, we assume that all tasks are performed according to the lexicographical ordering of $\text{order}(\mathbf{V})$, which is the standard implementation in `pcalg` (Kalisch et al., 2012) and TETRAD IV (Spirtes et al., 2000), and is called “PC-1” in Spirtes et al. (2000) (Section 5.4.2.4).

In Step 1, $\text{order}(\mathbf{V})$ affects the estimation of the *skeleton* and the *separating sets*. In particular, at each level of ℓ , $\text{order}(\mathbf{V})$ determines the order in which pairs of adjacent vertices and subsets \mathbf{S} of their adjacency sets are considered (see lines 6 and 8 in Algorithm 3.2). The skeleton \mathcal{C} is updated after each edge removal. Hence, the adjacency sets typically change within one level of ℓ , and this affects which other conditional independencies are checked, since the algorithm only conditions on subsets of the adjacency sets. In the oracle version, we have perfect conditional independence information, and all orderings on the variables lead to the same output. In the sample version, however, we typically make mistakes in keeping or removing edges. In such cases, the resulting changes in the adjacency sets can lead to different skeletons, as illustrated in Example 1.

Moreover, different variable orderings can lead to different separating sets in Step 1. In the oracle version, this is not important, because any valid separating set leads to the correct v-structure decision in Step 2. In the sample version, however, different separating sets in Step 1 of the algorithm may yield different decisions about v-structures in Step 2. This is illustrated in Example 2.

Finally, we consider the role of $\text{order}(\mathbf{V})$ on the *orientation rules* in Steps 2 and 3 of the sample version of the PC-algorithm. Example 3 illustrates that different variable

orderings can lead to different orientations, even if the skeleton and separating sets are order-independent.

Example 1 (*Order-dependent skeleton in the sample version of the PC-algorithm.*) Suppose that the distribution of $\mathbf{V} = \{X_1, X_2, X_3, X_4, X_5\}$ is faithful to the DAG in Figure 2(a). This DAG encodes the following conditional independencies with minimal separating sets: $X_1 \perp\!\!\!\perp X_2$ and $X_2 \perp\!\!\!\perp X_4 \mid \{X_1, X_3\}$.

Suppose that we have an i.i.d. sample of $(X_1, X_2, X_3, X_4, X_5)$, and that the following conditional independencies with minimal separating sets are judged to hold at some significance level α : $X_1 \perp\!\!\!\perp X_2$, $X_2 \perp\!\!\!\perp X_4 \mid \{X_1, X_3\}$, and $X_3 \perp\!\!\!\perp X_4 \mid \{X_1, X_5\}$. Thus, the first two are correct, while the third is false.

We now apply the PC-algorithm with two different orderings: $order_1(\mathbf{V}) = (X_1, X_4, X_2, X_3, X_5)$ and $order_2(\mathbf{V}) = (X_1, X_3, X_4, X_2, X_5)$. The resulting skeletons are shown in Figures 2(b) and 2(c), respectively. We see that the skeletons are different, and that both are incorrect as the edge $X_3 - X_4$ is missing. The skeleton for $order_2(\mathbf{V})$ contains an additional error, as there is an additional edge $X_2 - X_4$.

We now go through Algorithm 3.2 to see what happened. We start with a complete undirected graph on \mathbf{V} . When $\ell = 0$, variables are tested for marginal independence, and the algorithm correctly removes the edge between X_1 and X_2 . No other conditional independencies are found when $\ell = 0$ or $\ell = 1$. When $\ell = 2$, there are two pairs of vertices that are thought to be conditionally independent given a subset of size 2, namely the pairs (X_2, X_4) and (X_3, X_4) .

In $order_1(\mathbf{V})$, the pair (X_4, X_2) is considered first. The corresponding edge is removed, as $X_4 \perp\!\!\!\perp X_2 \mid \{X_1, X_3\}$ and $\{X_1, X_3\}$ is a subset of $adj(\mathcal{C}, X_4) = \{X_1, X_2, X_3, X_5\}$. Next, the pair (X_4, X_3) is considered and the corresponding edge is erroneously removed, because of the wrong decision that $X_4 \perp\!\!\!\perp X_3 \mid \{X_1, X_5\}$ and the fact that $\{X_1, X_5\}$ is a subset of $adj(\mathcal{C}, X_4) = \{X_1, X_3, X_5\}$.

In $order_2(\mathbf{V})$, the pair (X_3, X_4) is considered first, and the corresponding edge is erroneously removed. Next, the algorithm considers the pair (X_4, X_2) . The corresponding separating set $\{X_1, X_3\}$ is not a subset of $adj(\mathcal{C}, X_4) = \{X_1, X_2, X_5\}$, so that the edge $X_2 - X_4$ remains. Next, the algorithm considers the pair (X_2, X_4) . Again, the separating set $\{X_1, X_3\}$ is not a subset of $adj(\mathcal{C}, X_2) = \{X_3, X_4, X_5\}$, so that the edge $X_2 - X_4$ again remains. In other words, since (X_3, X_4) was considered first in $order_2(\mathbf{V})$, the adjacency set of X_4 was affected and no longer contained X_3 , so that the algorithm “forgot” to check the conditional independence $X_2 \perp\!\!\!\perp X_4 \mid \{X_1, X_3\}$.

Example 2 (*Order-dependent separating sets and v-structures in the sample version of the PC-algorithm.*) Suppose that the distribution of $\mathbf{V} = \{X_1, X_2, X_3, X_4, X_5\}$ is faithful to the DAG in Figure 3(a). This DAG encodes the following conditional independencies with minimal separating sets: $X_1 \perp\!\!\!\perp X_3 \mid \{X_2\}$, $X_1 \perp\!\!\!\perp X_4 \mid \{X_2\}$, $X_1 \perp\!\!\!\perp X_4 \mid \{X_3\}$, $X_2 \perp\!\!\!\perp X_4 \mid \{X_3\}$, $X_2 \perp\!\!\!\perp X_5 \mid \{X_1, X_3\}$, $X_2 \perp\!\!\!\perp X_5 \mid \{X_1, X_4\}$, $X_3 \perp\!\!\!\perp X_5 \mid \{X_1, X_4\}$ and $X_3 \perp\!\!\!\perp X_5 \mid \{X_2, X_4\}$.

We consider the oracle version of the PC-algorithm with two different orderings on the variables: $order_3(\mathbf{V}) = (X_1, X_4, X_2, X_3, X_5)$ and $order_4(\mathbf{V}) = (X_1, X_4, X_3, X_2, X_5)$. For $order_3(\mathbf{V})$, we obtain $sepset(X_1, X_4) = \{X_2\}$, while for $order_4(\mathbf{V})$ we get $sepset(X_1, X_4) =$

$\{X_3\}$. Thus, the separating sets are order-dependent. However, we obtain the same v -structure $X_1 \rightarrow X_5 \leftarrow X_4$ for both orderings, since X_5 is not in the $\text{sepset}(X_1, X_4)$, regardless of the ordering. In fact, this holds in general, since in the oracle version of the PC-algorithm, a vertex is either in all possible separating sets or in none of them (Spirtes et al., 2000, Lemma 5.1.3).

Now suppose that we have an i.i.d. sample of $(X_1, X_2, X_3, X_4, X_5)$. Suppose that at some significance level α , all true conditional independencies are judged to hold, and $X_1 \perp\!\!\!\perp X_3 \mid \{X_4\}$ is thought to hold by mistake. We again consider two different orderings: $\text{order}_5(\mathbf{V}) = (X_1, X_3, X_4, X_2, X_5)$ and $\text{order}_6(\mathbf{V}) = (X_3, X_1, X_2, X_4, X_5)$. With $\text{order}_5(\mathbf{V})$ we obtain the incorrect $\text{sepset}(X_1, X_3) = \{X_4\}$. This also leads to an incorrect v -structure $X_1 \rightarrow X_2 \leftarrow X_3$ in Step 2 of the algorithm. With $\text{order}_6(\mathbf{V})$, we obtain the correct $\text{sepset}(X_1, X_3) = \{X_2\}$, and hence correctly find that $X_1 - X_2 - X_3$ is not a v -structure in Step 2. This illustrates that order-dependent separating sets in Step 1 of the sample version of the PC-algorithm can lead to order-dependent v -structures in Step 2 of the algorithm.

Example 3 (Order-dependent orientation rules in Steps 2 and 3 of the sample version of the PC-algorithm.) Consider the graph in Figure 4(a) with unshielded triples (X_1, X_2, X_3) and (X_2, X_3, X_4) , and assume this is the skeleton after Step 1 of the sample version of the PC-algorithm. Moreover, assume that we found $\text{sepset}(X_1, X_3) = \text{sepset}(X_2, X_4) = \text{sepset}(X_1, X_4) = \emptyset$. Then in Step 2 of the algorithm, we obtain two v -structures $X_1 \rightarrow X_2 \leftarrow X_3$ and $X_2 \rightarrow X_3 \leftarrow X_4$. Of course this means that at least one of the statistical tests is wrong, but this can happen in the sample version. We now have conflicting information about the orientation of the edge $X_2 - X_3$. In the current implementation of `pcalg`, where conflicting edges are simply overwritten, this means that the orientation of $X_2 - X_3$ is determined by the v -structure that is last considered. Thus, we obtain $X_1 \rightarrow X_2 \rightarrow X_3 \leftarrow X_4$ if (X_2, X_3, X_4) is considered last, while we get $X_1 \rightarrow X_2 \leftarrow X_3 \leftarrow X_4$ if (X_1, X_2, X_3) is considered last.

Next, consider the graph in Figure 4(b), and assume that this is the output of the sample version of the PC-algorithm after Step 2. Thus, we have two v -structures, namely $X_1 \rightarrow X_2 \leftarrow X_3$ and $X_4 \rightarrow X_5 \leftarrow X_6$, and four unshielded triples, namely (X_1, X_2, X_5) , (X_3, X_2, X_5) , (X_4, X_5, X_2) , and (X_6, X_5, X_2) . Thus, we then apply the orientation rules in Step 3 of the algorithm, starting with rule R1. If one of the two unshielded triples (X_1, X_2, X_5) or (X_3, X_2, X_5) is considered first, we obtain $X_2 \rightarrow X_5$. On the other hand, if one of the unshielded triples (X_4, X_5, X_2) or (X_6, X_5, X_2) is considered first, then we obtain $X_2 \leftarrow X_5$. Note that we have no issues with overwriting of edges here, since as soon as the edge $X_2 - X_5$ is oriented, all edges are oriented and no further orientation rules are applied.

These examples illustrate that Steps 2 and 3 of the PC-algorithm can be order-dependent regardless of the output of the previous steps.

4. Modified Algorithms

We now propose several modifications of the PC-algorithm (and hence also of the related algorithms) that remove the order-dependence in the various stages of the algorithm. Sections 4.1, 4.2, and 4.3 discuss the skeleton, the v -structures and the orientation rules, respectively. In each of these sections, we first describe the oracle version of the modifications, and then

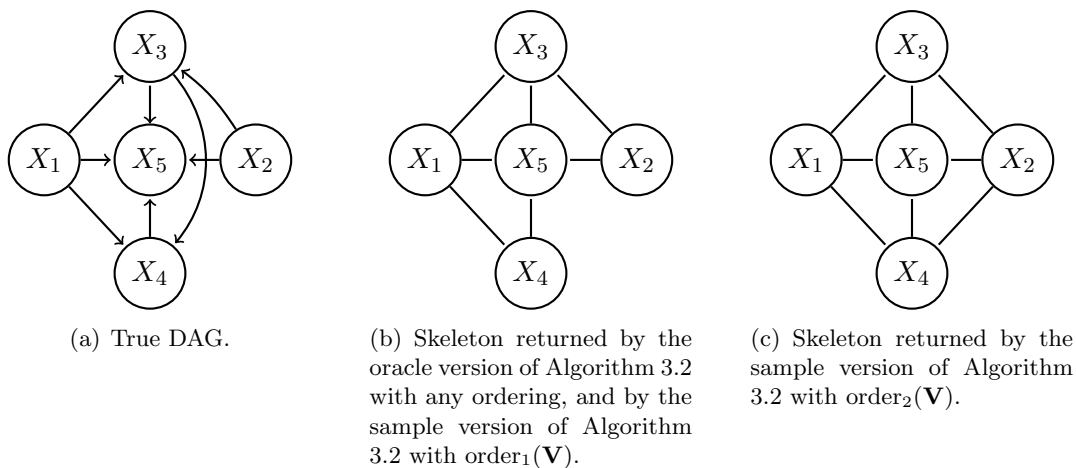


Figure 2: Graphs corresponding to Examples 1 and 4.

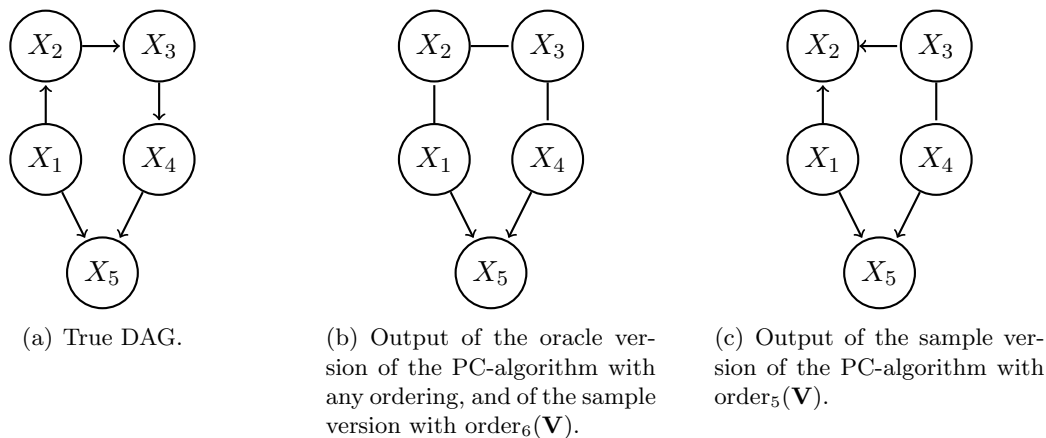


Figure 3: Graphs corresponding to Examples 2 and 5.

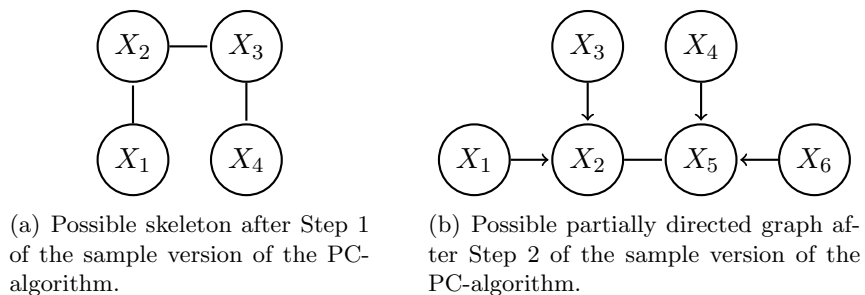


Figure 4: Graphs corresponding to Examples 3 and 6.

results and examples about order-dependence in the corresponding sample version (obtained by replacing conditional independence queries by conditional independence tests, as in Section 3.3). Finally, Section 4.4 discusses order-independent versions of related algorithms like RFCI and FCI, and Section 4.5 presents high-dimensional consistency results for the sample versions of all modifications.

4.1 The Skeleton

We first consider estimation of the skeleton in the adjacency search (Step 1) of the PC-algorithm. The pseudocode for our modification is given in Algorithm 4.1. The resulting PC-algorithm, where Step 1 in Algorithm 3.1 is replaced by Algorithm 4.1, is called “PC-stable”.

The main difference between Algorithms 3.2 and 4.1 is given by the for-loop on lines 6-8 in the latter one, which computes and stores the adjacency sets $a(X_i)$ of all variables after each new size ℓ of the conditioning sets. These stored adjacency sets $a(X_i)$ are used whenever we search for conditioning sets of this given size ℓ . Consequently, an edge deletion on line 13 no longer affects which conditional independencies are checked for other pairs of variables at this level of ℓ .

In other words, at each level of ℓ , Algorithm 4.1 records which edges should be removed, but for the purpose of the adjacency sets it removes these edges only when it goes to the next value of ℓ . Besides resolving the order-dependence in the estimation of the skeleton, our algorithm has the advantage that it is easily parallelizable at each level of ℓ .

The PC-stable algorithm is sound and complete in the oracle version (Theorem 2), and yields order-independent skeletons in the sample version (Theorem 3). We illustrate the algorithm in Example 4.

Theorem 2 *Let the distribution of \mathbf{V} be faithful to a DAG $\mathcal{G} = (\mathbf{V}, \mathbf{E})$, and assume that we are given perfect conditional independence information about all pairs of variables (X_i, X_j) in \mathbf{V} given subsets $\mathbf{S} \subseteq \mathbf{V} \setminus \{X_i, X_j\}$. Then the output of the PC-stable algorithm is the CPDAG that represents \mathcal{G} .*

Proof The proof of Theorem 2 is completely analogous to the proof of Theorem 1 for the original PC-algorithm, as discussed in Section 3.1. ■

Theorem 3 *The skeleton resulting from the sample version of the PC-stable algorithm is order-independent.*

Proof We consider the removal or retention of an arbitrary edge $X_i - X_j$ at some level ℓ . The ordering of the variables determines the order in which the edges (line 9 of Algorithm 4.1) and the subsets \mathbf{S} of $a(X_i)$ and $a(X_j)$ (line 11 of Algorithm 4.1) are considered. By construction, however, the order in which edges are considered does not affect the sets $a(X_i)$ and $a(X_j)$.

If there is at least one subset \mathbf{S} of $a(X_i)$ or $a(X_j)$ such that $X_i \perp\!\!\!\perp X_j | \mathbf{S}$, then any ordering of the variables will find a separating set for X_i and X_j (but different orderings may lead to different separating sets as illustrated in Example 2). Conversely, if there is no

Algorithm 4.1 Step 1 of the PC-stable algorithm (oracle version)

Require: Conditional independence information among all variables in \mathbf{V} , and an ordering $\text{order}(\mathbf{V})$ on the variables

- 1: Form the complete undirected graph \mathcal{C} on the vertex set \mathbf{V}
 - 2: Let $\ell = -1$;
 - 3: **repeat**
 - 4: Let $\ell = \ell + 1$;
 - 5: **for all** vertices X_i in \mathcal{C} **do**
 - 6: Let $a(X_i) = \text{adj}(\mathcal{C}, X_i)$
 - 7: **end for**
 - 8: **repeat**
 - 9: Select a (new) ordered pair of vertices (X_i, X_j) that are adjacent in \mathcal{C} and satisfy $|a(X_i) \setminus \{X_j\}| \geq \ell$, using $\text{order}(\mathbf{V})$;
 - 10: **repeat**
 - 11: Choose a (new) set $\mathbf{S} \subseteq a(X_i) \setminus \{X_j\}$ with $|\mathbf{S}| = \ell$, using $\text{order}(\mathbf{V})$;
 - 12: **if** X_i and X_j are conditionally independent given \mathbf{S} **then**
 - 13: Delete edge $X_i - X_j$ from \mathcal{C} ;
 - 14: Let $\text{sepset}(X_i, X_j) = \text{sepset}(X_j, X_i) = \mathbf{S}$;
 - 15: **end if**
 - 16: **until** X_i and X_j are no longer adjacent in \mathcal{C} or all $\mathbf{S} \subseteq a(X_i) \setminus \{X_j\}$ with $|\mathbf{S}| = \ell$ have been considered
 - 17: **until** all ordered pairs of adjacent vertices (X_i, X_j) in \mathcal{C} with $|a(X_i) \setminus \{X_j\}| \geq \ell$ have been considered
 - 18: **until** all pairs of adjacent vertices (X_i, X_j) in \mathcal{C} satisfy $|a(X_i) \setminus \{X_j\}| \leq \ell$
 - 19: **return** \mathcal{C} , sepset .
-

subset \mathbf{S}' of $a(X_i)$ or $a(X_j)$ such that $X_i \perp\!\!\!\perp X_j | \mathbf{S}'$, then no ordering will find a separating set.

Hence, any ordering of the variables leads to the same edge deletions, and therefore to the same skeleton. ■

Example 4 (*Order-independent skeletons*) We go back to Example 1, and consider the sample version of Algorithm 4.1. The algorithm now outputs the skeleton shown in Figure 2(b) for both orderings $\text{order}_1(\mathbf{V})$ and $\text{order}_2(\mathbf{V})$.

We again go through the algorithm step by step. We start with a complete undirected graph on \mathbf{V} . The only conditional independence found when $\ell = 0$ or $\ell = 1$ is $X_1 \perp\!\!\!\perp X_2$, and the corresponding edge is removed. When $\ell = 2$, the algorithm first computes the new adjacency sets: $a(X_1) = a(X_2) = \{X_3, X_4, X_5\}$ and $a(X_i) = \mathbf{V} \setminus \{X_i\}$ for $i = 3, 4, 5$. There are two pairs of variables that are thought to be conditionally independent given a subset of size 2, namely (X_2, X_4) and (X_3, X_4) . Since the sets $a(X_i)$ are not updated after edge removals, it does not matter in which order we consider the ordered pairs (X_2, X_4) , (X_4, X_2) , (X_3, X_4) and (X_4, X_3) . Any ordering leads to the removal of both edges, as the

separating set $\{X_1, X_3\}$ for (X_4, X_2) is contained in $a(X_4)$, and the separating set $\{X_1, X_5\}$ for (X_3, X_4) is contained in $a(X_3)$ (and in $a(X_4)$).

4.2 Determination of the V-structures

We propose two methods to resolve the order-dependence in the determination of the v-structures, using the conservative PC-algorithm (CPC) of Ramsey et al. (2006) and a variation thereof.

The CPC-algorithm works as follows. Let \mathcal{C} be the graph resulting from Step 1 of the PC-algorithm (Algorithm 3.1). For all unshielded triples (X_i, X_j, X_k) in \mathcal{C} , determine all subsets \mathbf{Y} of $\text{adj}(\mathcal{C}, X_i)$ and of $\text{adj}(\mathcal{C}, X_k)$ that make X_i and X_k conditionally independent, i.e., that satisfy $X_i \perp\!\!\!\perp X_k | \mathbf{Y}$. We refer to such sets as separating sets. The triple (X_i, X_j, X_k) is labelled as *unambiguous* if at least one such separating set is found and either X_j is in all separating sets or in none of them; otherwise it is labelled as *ambiguous*. If the triple is unambiguous, it is oriented as v-structure if and only if X_j is in none of the separating sets. Moreover, in Step 3 of the PC-algorithm (Algorithm 3.1), the orientation rules are adapted so that only unambiguous triples are oriented. The output of the CPC-algorithm is a partially directed graph in which ambiguous triples are marked.

We found that the CPC-algorithm can be very conservative, in the sense that very few unshielded triples are unambiguous in the sample version. We therefore propose a minor modification of this approach, called majority rule PC-algorithm (MPC). As in CPC, we first determine all subsets \mathbf{Y} of $\text{adj}(\mathcal{C}, X_i)$ and of $\text{adj}(\mathcal{C}, X_k)$ satisfying $X_i \perp\!\!\!\perp X_k | \mathbf{Y}$. We then label the triple (X_i, X_j, X_k) as *unambiguous* if at least one such separating set is found and X_j is not in exactly 50% of the separating sets. Otherwise it is labelled as *ambiguous*. (Of course, one can also use different cut-offs to declare ambiguous and non-ambiguous triples.) If a triple is unambiguous, it is oriented as v-structure if and only if X_j is in less than half of the separating sets. As in CPC, the orientation rules in Step 3 are adapted so that only unambiguous triples are oriented, and the output is a partially directed graph in which ambiguous triples are marked.

We refer to the combination of PC-stable and CPC/MPC as the CPC/MPC-stable algorithms. Theorem 4 states that the oracle versions of the CPC- and MPC-stable algorithms are sound and complete. When looking at the sample versions of the algorithms, we note that any unshielded triple that is judged to be unambiguous in CPC-stable is also unambiguous in MPC-stable, and any unambiguous v-structure in CPC-stable is an unambiguous v-structure in MPC-stable. In this sense, CPC-stable is more conservative than MPC-stable, although the difference appears to be small in simulations and for the yeast data (see Sections 5 and 6). Both CPC-stable and MPC-stable share the property that the determination of v-structures no longer depends on the (order-dependent) separating sets that were found in Step 1 of the algorithm. Therefore, both CPC-stable and MPC-stable yield order-independent decisions about v-structures in the sample version, as stated in Theorem 5. Example 5 illustrates both algorithms.

We note that the CPC/MPC-stable algorithms may yield a lot fewer directed edges than PC-stable. On the other hand, we can put more trust in those edges that were oriented.

Theorem 4 *Let the distribution of \mathbf{V} be faithful to a DAG $\mathcal{G} = (\mathbf{V}, \mathbf{E})$, and assume that we are given perfect conditional independence information about all pairs of variables (X_i, X_j)*

in \mathbf{V} given subsets $\mathbf{S} \subseteq \mathbf{V} \setminus \{X_i, X_j\}$. Then the output of the CPC/MPC(-stable) algorithms is the CPDAG that represents \mathcal{G} .

Proof The skeleton of the CPDAG is correct by Theorems 1 and 2. The unshielded triples are all unambiguous (in the conservative and the majority rule versions), since for any unshielded triple (X_i, X_j, X_k) in a DAG, X_j is either in all sets that d-separate X_i and X_k or in none of them (Spirtes et al., 2000, Lemma 5.1.3). In particular, this also means that all v-structures are determined correctly. Finally, since all unshielded triples are unambiguous, the orientation rules are as in the original oracle PC-algorithm, and soundness and completeness of these rules follows from Meek (1995) and Andersson et al. (1997). ■

Theorem 5 *The decisions about v-structures in the sample versions of the CPC/MPC-stable algorithms are order-independent.*

Proof The CPC/MPC-stable algorithms have order-independent skeletons in Step 1, by Theorem 3. In particular, this means that their unshielded triples and adjacency sets are order-independent. The decision about whether an unshielded triple is unambiguous and/or a v-structure is based on the adjacency sets of nodes in the triple, which are order-independent. ■

Example 5 (*Order-independent decisions about v-structures*) *We consider the sample versions of the CPC/MPC-stable algorithms, using the same input as in Example 2. In particular, we assume that all conditional independencies induced by the DAG in Figure 3(a) are judged to hold, plus the additional (erroneous) conditional independency $X_1 \perp\!\!\!\perp X_3 | X_4$.*

Denote the skeleton after Step 1 by \mathcal{C} . We consider the unshielded triple (X_1, X_2, X_3) . First, we compute $\text{adj}(\mathcal{C}, X_1) = \{X_2, X_5\}$ and $\text{adj}(\mathcal{C}, X_3) = \{X_2, X_4\}$. We now consider all subsets \mathbf{Y} of these adjacency sets, and check whether $X_1 \perp\!\!\!\perp X_3 | \mathbf{Y}$. The following separating sets are found: $\{X_2\}$, $\{X_4\}$, and $\{X_2, X_4\}$.

Since X_2 is in some but not all of these separating sets, CPC-stable determines that the triple is ambiguous, and no orientations are performed. Since X_2 is in more than half of the separating sets, MPC-stable determines that the triple is unambiguous and not a v-structure. The output of both algorithms is given in Figure 3(b).

4.3 Orientation Rules

Even when the skeleton and the determination of the v-structures are order-independent, Example 3 showed that there might be some order-dependence left in the sample-version. This can be resolved by allowing bi-directed edges (\leftrightarrow) and working with lists containing the candidate edges for the v-structures in Step 2 and the orientation rules R1-R3 in Step 3.

In particular, in Step 2 we generate a list of all (unambiguous) v-structures, and then orient all of these, creating a bi-directed edge in case of a conflict between two v-structures. In Step 3, we first generate a list of all edges that can be oriented by rule R1. We orient all

these edges, again creating bi-directed edges if there are conflicts. We do the same for rules R2 and R3, and iterate this procedure until no more edges can be oriented.

When using this procedure, we add the letter L (standing for lists), e.g., LCPC-stable and LMPC-stable. The LCPC-stable and LMPC-stable algorithms are correct in the oracle version (Theorem 6) and fully order-independent in the sample versions (Theorem 7). The procedure is illustrated in Example 6.

We note that the bi-directed edges cannot be interpreted causally. They simply indicate that there was some conflicting information in the algorithm.

Theorem 6 *Let the distribution of \mathbf{V} be faithful to a DAG $\mathcal{G} = (\mathbf{V}, \mathbf{E})$, and assume that we are given perfect conditional independence information about all pairs of variables (X_i, X_j) in \mathbf{V} given subsets $\mathbf{S} \subseteq \mathbf{V} \setminus \{X_i, X_j\}$. Then the (L)CPC(-stable) and (L)MPC(-stable) algorithms output the CPDAG that represents \mathcal{G} .*

Proof By Theorem 4, we know that the CPC(-stable) and MPC(-stable) algorithms are correct. With perfect conditional independence information, there are no conflicts between v-structures in Step 2 of the algorithms, nor between orientation rules in Step 3 of the algorithms. Therefore, the (L)CPC(-stable) and (L)MPC(-stable) algorithms are identical to the CPC(-stable) and MPC(-stable) algorithms. ■

Theorem 7 *The sample versions of LCPC-stable and LMPC-stable are fully order-independent.*

Proof This follows straightforwardly from Theorems 3 and 5 and the procedure with lists and bi-directed edges discussed above. ■

Table 1 summarizes the three order-dependence issues explained above and the corresponding modifications of the PC-algorithm that removes the given order-dependence problem.

	skeleton	v-structures decisions	edges orientations
PC	-	-	-
PC-stable	✓	-	-
CPC/MPC-stable	✓	✓	-
BCPC/BMPC-stable	✓	✓	✓

Table 1: Order-dependence issues and corresponding modifications of the PC-algorithm that remove the problem. A tick mark indicates that the corresponding aspect of the graph is estimated order-independently in the sample version. For example, with PC-stable the skeleton is estimated order-independently but not the v-structures and the edge orientations.

Example 6 *First, we consider the two unshielded triples (X_1, X_2, X_3) and (X_2, X_3, X_4) as shown in Figure 4(a). The version of the algorithm that uses lists for the orientation rules, orients these edges as $X_1 \rightarrow X_2 \leftrightarrow X_3 \leftarrow X_4$, regardless of the ordering of the variables.*

Next, we consider the structure shown in Figure 4(b). As a first step, we construct a list containing all candidate structures eligible for orientation rule R1 in Step 3. The list contains the unshielded triples (X_1, X_2, X_5) , (X_3, X_2, X_5) , (X_4, X_5, X_2) , and (X_6, X_5, X_2) . Now, we go through each element in the list and we orient the edges accordingly, allowing bi-directed edges. This yields the edge orientation $X_2 \leftrightarrow X_5$, regardless of the ordering of the variables.

4.4 Related Algorithms

If there are unmeasured common causes or unmeasured selection variables, which is often the case in practice, then causal inference based on the PC-algorithm may be incorrect. In such cases, one needs a generalization of a DAG, called a maximal ancestral graph (MAG) (Richardson and Spirtes, 2002). A MAG describes causal information in its edge marks, and entails conditional independence relationships via *m-separation* (Richardson and Spirtes, 2002), a generalization of d-separation. Several MAGs can describe exactly the same conditional independence information. Such MAGs are called Markov equivalent and form a Markov equivalence class, which can be represented by a partial ancestral graph (PAG) (Richardson and Spirtes, 2002; Ali et al., 2009). PAGs describe causal features common to every MAG in the Markov equivalence class, and hence to every DAG (possibly with latent and selection variables) compatible with the observable independence structure under the assumption of faithfulness. More information on the interpretation of MAGs and PAGs can be found in, e.g., Colombo et al. (2012) (Sections 1.2 and 2.2).

PAGs can be learned by the FCI-algorithm (Spirtes et al., 2000, 1999). As a first step, this algorithm runs Steps 1 and 2 of the PC-algorithm (Algorithm 3.1). Based on the resulting graph, it then computes certain sets, called “Possible-D-SEP” sets, and conducts more conditional independence tests given subsets of the Possible-D-SEP sets. This can lead to additional edge removals and corresponding separating sets. After this, the v-structures are newly determined. Finally, there are ten orientation rules as defined by Zhang (2008). The output of the FCI-algorithm is an (estimated) PAG (Colombo et al., 2012, Definition 3.1).

From our results, it immediately follows that FCI with any of our modifications of the PC-algorithm is sound and complete in the oracle version. Moreover, we can easily construct partially or fully order-independent sample versions as follows. To solve the order-dependence in the skeleton we can use the following three step approach. First, we use PC-stable to find an initial order-independent skeleton. Next, since Possible-D-SEP sets are determined from the orientations of the v-structures, we need order-independent v-structures. Therefore, in Step 2 we can determine the v-structures using CPC. Finally, we compute the Possible-D-SEP sets for all pairs of nodes at once, and do not update these after possible edge removals. The modification that uses these three steps returns an order-independent skeleton, and we call it FCI-stable. To assess order-independent v-structures in the final output, one should again use an order-independent procedure, as in CPC or MPC for the second time that v-structures are determined. We call these modifications

CFCI-stable and MFCI-stable, respectively. Regarding the orientation rules, we note that the FCI-algorithm does not suffer from conflicting v -structures (as shown in Figure 4(a) for the PC-algorithm), because it orients edge *marks* and because bi-directed edges are allowed. However, the ten orientation rules still suffer from order-dependence issues as in the PC-algorithm (see Example 3 and Figure 4(b)). To solve this problem, we can again use lists of candidate edges for each orientation rule as explained in the previous section about the PC-algorithm. We refer to these modifications as LCFCI-stable and LMFCI-stable, and they are fully order-independent in the sample version. However, since these ten orientation rules are more involved than the three for PC, using lists can be very slow for some rules, for example the one for discriminating paths.

Table 2 summarizes the three order-dependence issues for FCI and the corresponding modifications that remove them.

	skeleton	v -structures decisions	edges orientations
FCI	-	-	-
FCI-stable	✓	-	-
CFCI/MFCI-stable	✓	✓	-
LCFCI/LMFCI-stable	✓	✓	✓

Table 2: Order-dependence issues and corresponding modifications of the FCI-algorithm that remove the problem. A tick mark indicates that the corresponding aspect of the graph is estimated order-independently in the sample version. For example, with FCI-stable the skeleton is estimated order-independently but not the v -structures and the edge orientations.

In the presences of latent and selection variables, one can also use the RFCI-algorithm (Colombo et al., 2012). This algorithm can be viewed as a compromise between PC and FCI, in the sense that its computational complexity is of the same order as PC, but its output can be interpreted causally without assuming causal sufficiency (but is slightly less informative than the output from FCI).

RFCI works as follows. It starts with the first step of PC. It then has a more involved Step 2 to determine the v -structures (Colombo et al., 2012, Lemma 3.1). In particular, for any unshielded triple (X_i, X_j, X_k) , it conducts additional tests to check if both X_i and X_j and X_j and X_k are conditionally dependent given $\text{sepset}(X_i, X_j) \setminus \{X_j\}$ found in Step 1. If a conditional independence relationship is detected, the corresponding edge is removed and a minimal separating set is stored. The removal of an edge can create new unshielded triples or destroy some of them. Therefore, the algorithm works with lists to make sure that these actions are order-independent. On the other hand, if both conditional dependencies hold and X_j is not in the separating set for (X_i, X_k) , the triple is oriented as a v -structure. Finally, in Step 3 it uses the ten orientation rules of Zhang (2008) with a modified orientation rule for the discriminating paths, that also involves some additional conditional independence tests. The output of the RFCI-algorithm is an (estimated) RFCI-PAG (Colombo et al., 2012, Definition 3.2).

From our results, it immediately follows that RFCI with any of our modifications of the PC-algorithm is correct in the oracle version, in the sense it outputs the true RFCI-PAG. Because of its more involved rules for v-structures and discriminating paths, one needs to make several adaptations to create a fully order-independent algorithm. For example, the additional conditional independence tests conducted for the v-structures are based on the separating sets found in Step 1. As already mentioned before (see Example 2) these separating sets are order-dependent, and therefore also the possible edge deletions based on them are order-dependent, leading to an order-dependent skeleton. To produce an order-independent skeleton one should use a similar approach to the conservative one for the v-structures to make the additional edge removals order-independent. Nevertheless, we can remove a large amount of the order-dependence in the skeleton by using the stable version for the skeleton as a first step. We refer to this modification as RFCI-stable. Note that this procedure does not produce a fully order-independent skeleton, but as shown in Section 5.2, it reduces the order-dependence considerably. Moreover, we can combine this modification with CPC or MPC on the final skeleton to reduce the order-dependence of the v-structures. We refer to these modifications as CRFCI-stable and MRFCI-stable. Finally, we can again use lists for the orientation rules as in the FCI-algorithm to reduce the order-dependence caused by the orientation rules.

Finally, in the presence of directed cycles, one can use the CCD-algorithm (Richardson, 1996). This algorithm can also be made order-independent using a similar approach.

4.5 High-Dimensional Consistency

The original PC-algorithm has been shown to be consistent for certain sparse high-dimensional graphs. In particular, Kalisch and Bühlmann (2007) proved consistency for multivariate Gaussian distributions. More recently, Harris and Drton (2013) showed consistency for the broader class of Gaussian copulas when using rank correlations, under slightly different conditions.

These high-dimensional consistency results allow the DAG \mathcal{G} and the number of observed variables p in \mathbf{V} to grow as a function of the sample size, so that $p = p_n$, $\mathbf{V} = \mathbf{V}_n = (X_{n,1}, \dots, X_{n,p_n})$ and $\mathcal{G} = \mathcal{G}_n$. The corresponding CPDAGs that represent \mathcal{G}_n are denoted by \mathcal{C}_n , and the estimated CPDAGs using tuning parameter α_n are denoted by $\hat{\mathcal{C}}_n(\alpha_n)$. Then the consistency results say that, under some conditions, there exists a sequence α_n such that $P(\hat{\mathcal{C}}_n(\alpha_n) = \mathcal{C}_n) \rightarrow 1$ as $n \rightarrow \infty$.

These consistency results rely on the fact that the PC-algorithm only performs conditional independence tests between pairs of variables given subsets \mathbf{S} of size less than or equal to the degree of the graph (when no errors are made). We made sure that our modifications still obey this property, and therefore the consistency results of Kalisch and Bühlmann (2007) and Harris and Drton (2013) remain valid for the (L)CPC(-stable) and (L)MPC(-stable) algorithms, under exactly the same conditions as for the original PC-algorithm.

Finally, also the consistency results of Colombo et al. (2012) for the FCI- and RFCI-algorithms remain valid for the (L)CFCI(-stable), (L)MFCI(-stable), CRFCI(-stable), and MRFCI(-stable) algorithms, under exactly the same conditions as for the original FCI- and RFCI-algorithms.

5. Simulations

We compared all algorithms on simulated data from low-dimensional and high-dimensional systems with and without latent variables. In the low-dimensional setting, we compared the modifications of PC, FCI and RFCI. All algorithms performed similarly in this setting, and the results are presented in Appendix A.1. The remainder of this section therefore focuses on the high-dimensional setting, where we compared (L)PC(-stable), (L)CPC(-stable) and (L)MPC(-stable) in systems without latent variables, and RFCI(-stable), CRFCI(-stable) and MRFCI(-stable) in systems with latent variables. We omitted the FCI-algorithm and the modifications with lists for the orientation rules of RFCI because of their computational complexity. Our results show that our modified algorithms perform better than the original algorithms in the high-dimensional settings we considered.

In Section 5.1 we describe the simulation setup. Section 5.2 evaluates the estimation of the skeleton of the CPDAG or PAG (i.e., only looking at the presence or absence of edges), and Section 5.3 evaluates the estimation of the CPDAG or PAG (i.e., also including the edge marks). Appendix A.2 compares the computing time and the number of conditional independence tests performed by PC and PC-stable, showing that PC-stable generally performs more conditional independence tests, and is slightly slower than PC. Finally, Appendix A.3 compares the modifications of FCI and RFCI in two medium-dimensional settings with latent variables, where the number of nodes in the graph is roughly equal to the sample size and we allow somewhat denser graphs. The results indicate that also in this setting our modified versions perform better than the original ones.

5.1 Simulation Setup

We used the following procedure to generate a random weighted DAG with a given number of vertices p and an expected neighborhood size $E(N)$. First, we generated a random adjacency matrix A with independent realizations of Bernoulli($E(N)/(p-1)$) random variables in the lower triangle of the matrix and zeroes in the remaining entries. Next, we replaced the ones in A by independent realizations of a Uniform($[0.1, 1]$) random variable, where a nonzero entry A_{ij} can be interpreted as an edge from X_j to X_i with weight A_{ij} . (We bounded the edge weights away from zero to avoid problems with near-unfaithfulness.)

We related a multivariate Gaussian distribution to each DAG by letting $X_1 = \epsilon_1$ and $X_i = \sum_{r=1}^{i-1} A_{ir} X_r + \epsilon_i$ for $i = 2, \dots, p$, where $\epsilon_1, \dots, \epsilon_p$ are mutually independent $\mathcal{N}(0, 1)$ random variables. The variables X_1, \dots, X_p then have a multivariate Gaussian distribution with mean zero and covariance matrix $\Sigma = (\mathbf{1} - A)^{-1}(\mathbf{1} - A)^{-T}$, where $\mathbf{1}$ is the $p \times p$ identity matrix.

We generated 250 random weighted DAGs with $p = 1000$ and $E(N) = 2$, and for each weighted DAG we generated an i.i.d. sample of size $n = 50$. The settings were chosen to somewhat resemble the observational yeast gene expression data (see Section 6). In the setting without latents, we simply used all variables. In the setting with latents, we removed half of the variables that had no parents and at least two children, chosen at random.

We estimated each graph for 20 random variable orderings, using the sample versions of (L)PC(-stable), (L)CPC(-stable), and (L)MPC(-stable) in the setting without latents, and the sample versions of RFCI(-stable), CRFCI(-stable), and MRFCI(-stable) in the setting with latents, with tuning parameter $\alpha \in \{0.000625, 0.00125, 0.0025, 0.005, 0.01, 0.02, 0.04\}$.

Thus, from each randomly generated DAG, we obtained 20 estimated CPDAGs or RFCI-PAGs from each algorithm, for each value of α .

5.2 Estimation of the Skeleton

Figure 5 shows the number of edges, the number of errors, and the true discovery rate for the estimated skeletons, when compared to the true CPDAG or true PAG. The figure only compares PC and PC-stable in the setting without latent variables, and RFCI and RFCI-stable in the setting with latent variables, since the modifications for the v-structures and the orientation rules do not affect the estimation of the skeleton.

We first consider the number of estimated errors in the skeleton, shown in the first row of Figure 5. We see that PC-stable and RFCI-stable return estimated skeletons with fewer edges than PC and RFCI, for all values of α . This can be explained by the fact that PC-stable and RFCI-stable tend to perform more tests than PC and RFCI (see also Appendix A.2). Moreover, for all algorithms smaller values of α lead to sparser outputs, as expected. When interpreting these plots, it is useful to know that the average number of edges in the true CPDAGs and PAGs is about 1000. Thus, for all algorithms and almost all values of α , the estimated graphs are too sparse.

The second row of Figure 5 shows that PC-stable and RFCI-stable make fewer errors in the estimation of the skeletons than PC and RFCI, for all values of α . This may be somewhat surprising given the observations above: for most values of α the output of PC and RFCI is too sparse, and the output of PC-stable and RFCI-stable is even sparser. Thus, it must be that PC-stable and RFCI-stable yield a large decrease in the number of false positive edges that outweighs any increase in false negative edges.

This conclusion is also supported by the last row of Figure 5, which shows that PC-stable and RFCI-stable have a better True Discovery Rate (TDR) for all values of α , where the TDR is defined as the proportion of edges in the estimated skeleton that are also present in the true skeleton.

Figure 6 shows more detailed results for the estimated skeletons of PC and PC-stable for one of the 250 graphs (randomly chosen), for four different values of α . For each value of α shown, PC yielded a certain number of stable edges that were present for all 20 variable orderings, but also a large number of extra edges that seem to pop in or out randomly for different orderings. The PC-stable algorithm yielded far fewer edges (shown in red), and roughly captured the edges that were stable among the different variable orderings for PC. The results for RFCI and RFCI-stable show an equivalent picture.

5.3 Estimation of the CPDAGs and PAGs

We now consider estimation of the CPDAG or PAG, that is, also taking into account the edge orientations. For CPDAGs, we summarize the number of estimation errors using the Structural Hamming Distance (SHD), which is defined as the minimum number of edge insertions, deletions, and flips that are needed in order to transform the estimated graph into the true one. For PAGs, we summarize the number of estimation errors by counting the number of errors in the edge marks, which we call “SHD edge marks”. For example, if an edge $X_i \rightarrow X_j$ is present in the estimated PAG but the true PAG contains $X_i \leftrightarrow X_j$,

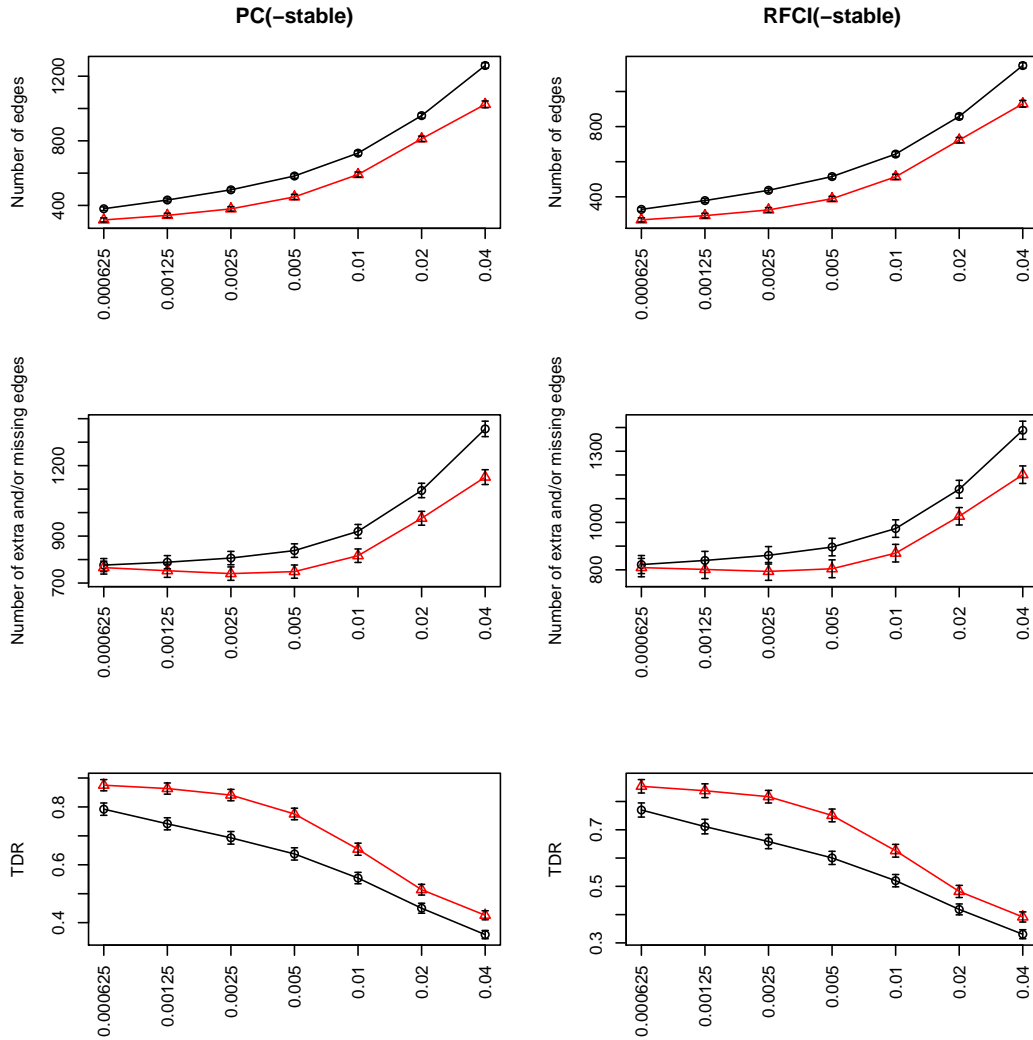


Figure 5: Estimation performance of PC (circles; black line) and PC-stable (triangles; red line) for the skeleton of the CPDAGs (first column of plots), and of RFCI (circles; black line) and RFCI-stable (triangles; red line) for the skeleton of the PAGs (second column of plots), for different values of α (x -axis displayed in log scale). The results are shown as averages plus or minus one standard deviation, computed over 250 randomly generated graphs and 20 random variable orderings per graph. The average number of edges in the true underlying CPDAGs and PAGs is about 1000.

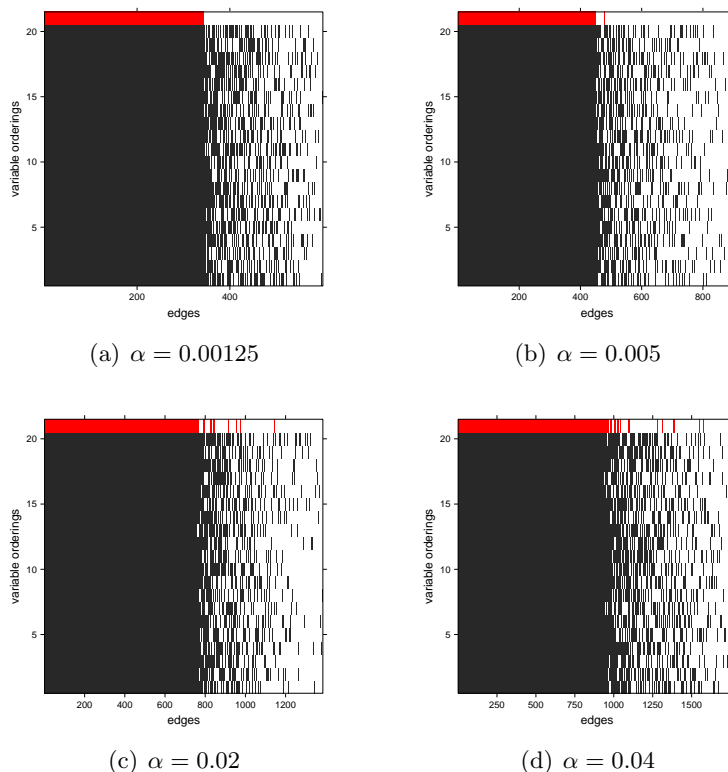


Figure 6: Estimated edges with the PC-algorithm (black) for 20 random orderings on the variables, as well as with the PC-stable algorithm (red, shown as variable ordering 21), for a random graph from the high-dimensional setting. The edges along the x -axes are ordered according to their presence in the 20 random orderings using the original PC-algorithm. Edges that did not occur for any of the orderings were omitted.

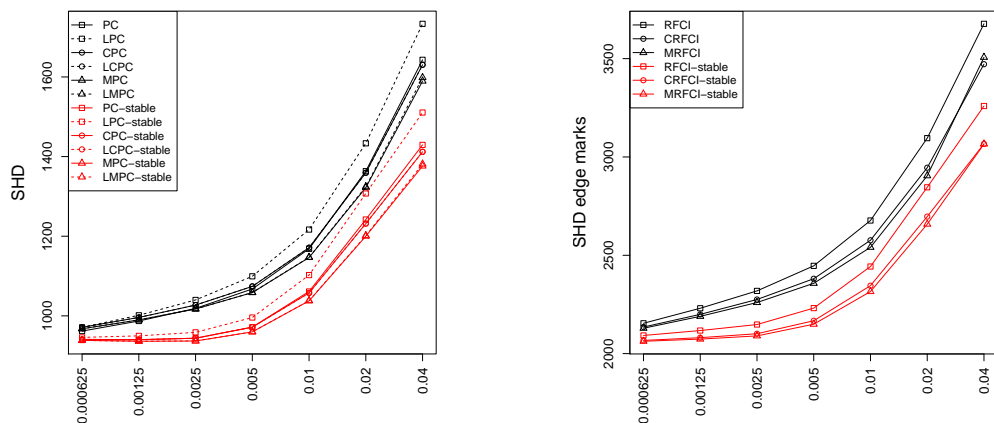
then that counts as one error, while it counts as two errors if the true PAG contains, for example, $X_i \leftarrow X_j$ or X_i and X_j are not adjacent.

Figure 7 shows that the PC-stable and RFCI-stable versions have significantly better estimation performance than the versions with the original skeleton, for all values of α . Moreover, MPC(-stable) and CPC(-stable) perform better than PC(-stable), as do MRFCI(-stable) and CRFCI(-stable) with respect to RFCI(-stable). Finally, for PC the idea to introduce bi-directed edges and lists in LCPC(-stable) and LMPC(-stable) seems to make little difference.

Figure 8 shows the variance in SHD for the CPDAGs, see Figure 8(a), and the variance in SHD edge marks for the PAGs, see Figure 8(b), both computed over the 20 random variable orderings per graph, and then plotted as averages over the 250 randomly generated graphs for the different values of α . The PC-stable and RFCI-stable versions yield significantly smaller variances than their counterparts with unstabilized skeletons. More-

over, the variance is further reduced for (L)CPC-stable and (L)MPC-stable, as well as for CRFCI-stable and MRFCI-stable, as expected.

Figure 9 shows receiver operating characteristic curves (ROC) for the directed edges in the estimated CPDAGs (Figure 9(a)) and PAGs (Figure 9(b)). We see that finding directed edges is much harder in settings that allow for hidden variables, as shown by the lower true positive rates (TPR) and higher false positive rates (FPR) in Figure 9(b). Within each figure, the different versions of the algorithms perform roughly similar, and MPC-stable and MRFCI-stable yield the best ROC-curves.



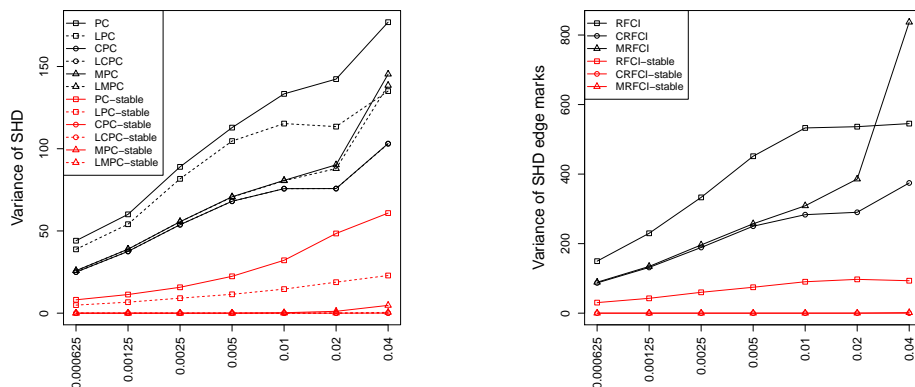
(a) Estimation performance of (L)PC(-stable), (L)CPC(-stable), and (L)MPC(-stable) for the CPDAGs in terms of SHD.

(b) Estimation performance of RFCI(-stable), CRFCI(-stable), and MRFCI(-stable) for the PAGs in terms of SHD edge marks.

Figure 7: Estimation performance in terms of SHD for the CPDAGs and SHD edge marks for the PAGs, shown as averages over 250 randomly generated graphs and 20 random variable orderings per graph, for different values of α (x -axis displayed in log scale).

6. Yeast Gene Expression Data

We also compared the PC and PC-stable algorithms on the yeast gene expression data (Hughes et al., 2000) that were already briefly discussed in Section 1. We recall that we chose these data since they contain both observational and experimental data, obtained under similar conditions. The observational data consist of gene expression measurements of 5361 genes for 63 wild-type cultures (observational data of size 63×5361). The experimental data consist of gene expression measurements of the same 5361 genes for 234 single-gene deletion mutant strains (experimental data of size 234×5361).



(a) Estimation performance of (L)PC(-stable), (L)CPC(-stable), and (L)MPC(-stable) for the CPDAGs in terms of the variance of SHD.

(b) Estimation performance of RFCI(-stable), CRFCI(-stable), and MRFCI(-stable) for the PAGs in terms of the variance SHD edge marks.

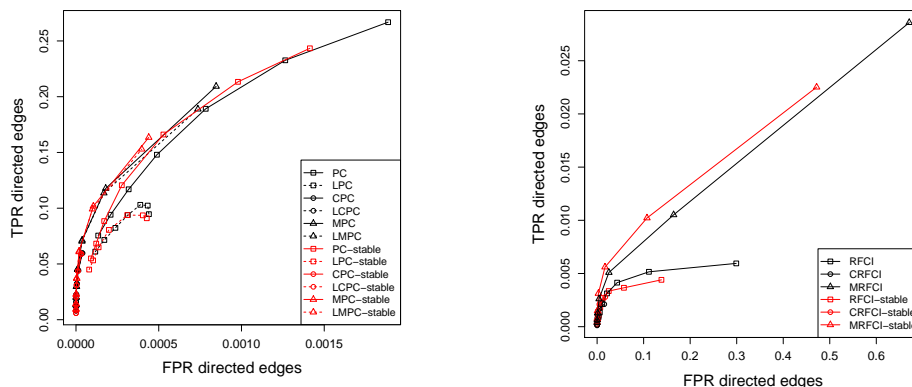
Figure 8: Estimation performance in terms of the variance of the SHD for the CPDAGs and SHD edge marks for the PAGs over the 20 random variable orderings per graph, shown as averages over 250 randomly generated graphs, for different values of α (x -axis displayed in log scale).

In Section 6.1 we consider estimation of the skeleton of the CPDAG, and in Section 6.2 we consider estimation of bounds on causal effects. We used the same data pre-processing as in Maathuis et al. (2010).

6.1 Estimation of the Skeleton

We applied PC and PC-stable to the (pre-processed) observational data. We saw in Section 1 that the PC-algorithm yielded estimated skeletons that were highly dependent on the variable ordering, as shown in black in Figure 10 for the 26 variable orderings (the original ordering and 25 random orderings of the variables). The PC-stable algorithm does not suffer from this order-dependence, and consequently all these 26 random orderings over the variables produce the same skeleton which is shown in the figure in red. We see that the PC-stable algorithm yielded a far sparser skeleton (2086 edges for PC-stable versus 5015-5159 edges for the PC-algorithm, depending on the variable ordering). Just as in the simulations in Section 5 the order-independent skeleton from the PC-stable algorithm roughly captured the edges that were stable among the different order-dependent skeletons estimated from different variable orderings for the original PC-algorithm.

To make “captured the edges that were stable” somewhat more precise, we defined the following two sets: Set 1 contained all edges (directed edges) that were present for all 26 variable orderings using the original PC-algorithm, and Set 2 contained all edges (directed edges) that were present for at least 90% of the 26 variable orderings using the original



(a) Estimation performance of (L)PC(-stable), (L)CPC(-stable), and (L)MPC(-stable) for the CPDAGs in terms of TPR and FPR for the directed edges.

(b) Estimation performance of RFCI(-stable), CRFCI(-stable), and MRFCI(-stable) for the PAGs in terms of TPR and FPR for the directed edges.

Figure 9: Estimation performance in terms of TPR and FPR for the directed edges in CPDAGs and PAGs, shown as averages over 250 randomly generated graphs and 20 random variable orderings per graph, where every curve is plotted with respect to the different values of α .

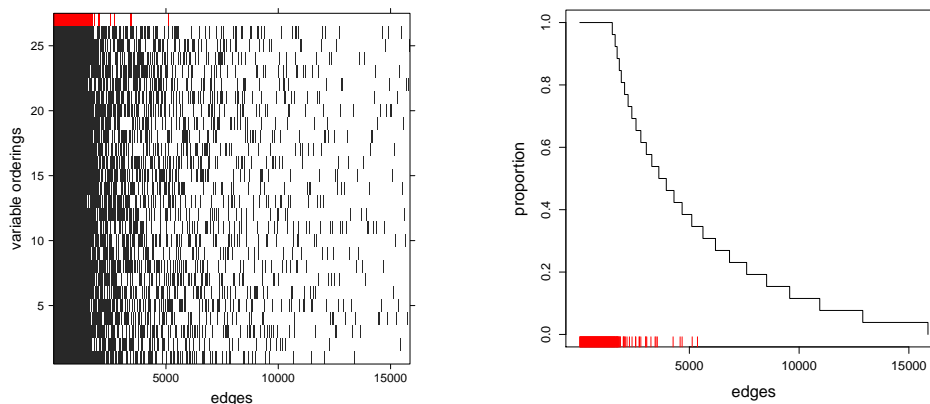
PC-algorithm. Set 1 contained 1478 edges (7 directed edges), while Set 2 contained 1700 edges (20 directed edges).

Table 3 shows how well the PC and PC-stable algorithms could find these stable edges in terms of number of edges in the estimated graphs that are present in Sets 1 and 2 (IN), and the number of edges in the estimated graphs that are not present in Sets 1 and 2 (OUT). We see that the number of estimated edges present in Sets 1 and 2 is about the same for both algorithms, while the output of the PC-stable algorithm has far fewer edges which are not present in the two specified sets.

Throughout our analyses of the yeast data, we used tuning parameter $\alpha = 0.01$, as in Maathuis et al. (2010). We are not aware of any fully satisfactory method to choose α in practice. In Appendix B, we briefly mention two possibilities that were described in Maathuis et al. (2009): optimizing a Bayesian Information Criterion (BIC) and stability selection (Meinshausen and Bühlmann, 2010).

6.2 Estimation of Causal Effects

We used the experimental data as the gold standard for estimating the total causal effects of the 234 deleted genes on the remaining 5361 (Maathuis et al., 2010). We then defined the top 10% of the largest effects in absolute value as the target set of effects, and we evaluated how well IDA (Maathuis et al., 2009, 2010) identified these effects from the observational data.



(a) As Figure 1(a), plus the edges occurring in the unique estimated skeleton using the PC-stable algorithm over the same 26 variable orderings (red, shown as variable ordering 27).

(b) The step function shows the proportion of the 26 variable orderings in which the edges were present for the original PC-algorithm, where the edges are ordered as in Figure 10(a). The red bars show the edges present in the estimated skeleton using the PC-stable algorithm.

Figure 10: Analysis of estimated skeletons of the CPDAGs for the yeast gene expression data (Hughes et al., 2000), using the PC and PC-stable algorithms with tuning parameter $\alpha = 0.01$. The PC-stable algorithm yields an order-independent skeleton that roughly captures the edges that were stable among the different variable orderings for the original PC-algorithm.

		Edges		Directed edges	
		PC	PC-stable	PC	PC-stable
Set 1	IN	1478 (0)	1478 (0)	7 (0)	7 (0)
	OUT	3606 (38)	607 (0)	4786 (47)	1433 (7)
Set 2	IN	1688 (3)	1688 (0)	19 (1)	20 (0)
	OUT	3396 (39)	397 (0)	4774 (47)	1420 (7)

Table 3: Number of edges in the estimated graphs that are present in Sets 1 and 2 (IN), and the number of edges in the estimated graphs that are not present in Sets 1 and 2 (OUT). The results are shown as averages (standard deviations) over the 26 variable orderings.

Figure 1(b) showed that IDA with the original PC-algorithm is highly order-dependent. Figure 11 shows the same analysis with PC-stable (solid black lines). We see that using PC-stable generally yielded better and more stable results than the original PC-algorithm. Note that some of the curves for PC-stable are worse than the reference curve of Maathuis et al. (2010) towards the beginning of the curves. This can be explained by the fact that the original variable ordering seems to be especially “lucky” for this part of the curve (see Figure 1(b)). There is still variability in the ROC curves in Figure 11 due to the order-dependent v-structures (because of order-dependent separating sets) and orientations in the PC-stable algorithm, but this variability is less prominent than in Figure 1(b). Finally, we see that there are 3 curves that produce a very poor fit.

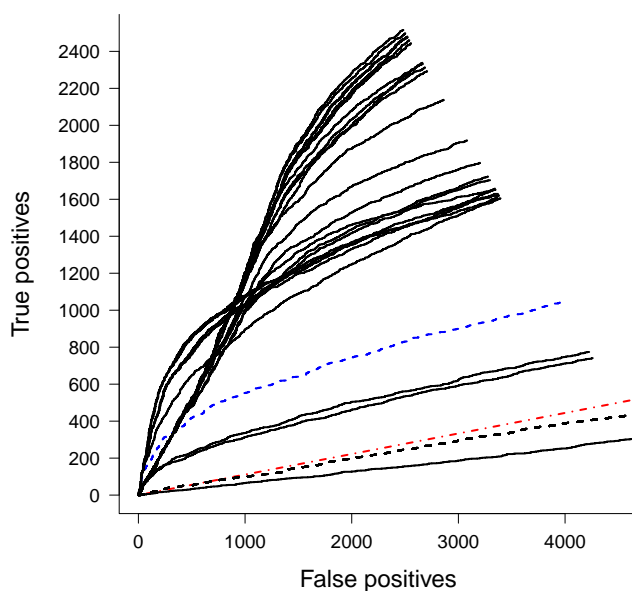


Figure 11: ROC curves corresponding to the 25 random orderings of the variables for the analysis of yeast gene expression data (Hughes et al., 2000), where the curves are generated as in Maathuis et al. (2010) but using PC-stable (solid black lines) and MPC-stable and CPC-stable (dashed black lines) with $\alpha = 0.01$. The ROC curves from Maathuis et al. (2010) (dashed blue) and the one for random guessing (dashed-dotted red) are shown as references. The resulting causal rankings are less order-dependent.

Using CPC-stable and MPC-stable helps in stabilizing the outputs, and in fact all the 25 random variable orderings produce almost the same CPDAGs for both modifications. Unfortunately, these estimated CPDAGs are almost entirely undirected (around 90 directed edges among the 2086 edges) which leads to a large equivalence class and consequently to a poor performance in IDA, see the dashed black line in Figure 11 which corresponds to the 25 random variable orderings for both CPC-stable and MPC-stable algorithms.

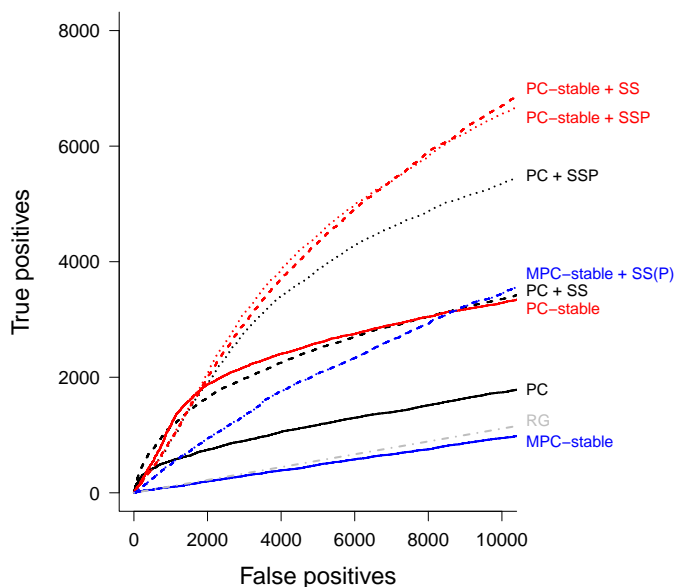


Figure 12: Analysis of the yeast gene expression data (Hughes et al., 2000) for PC, PC-stable, and MPC-stable algorithms using the original ordering over the variables (solid lines), using 100 runs stability selection without permuting the variable orderings, labelled as + SS (dashed lines), and using 100 runs stability selection with permuting the variable orderings, labelled as + SSP (dotted lines). The grey line labelled as RG represents the random guessing.

Another possible solution for the order-dependence orientation issues would be to use stability selection (Meinshausen and Bühlmann, 2010) to find the most stable orientations among the runs. In fact, Stekhoven et al. (2012) already proposed a combination of IDA and stability selection which led to improved performance when compared to IDA alone, but they used the original PC-algorithm and did not permute the variable ordering. We present here a more extensive analysis, where we consider the PC-algorithm (black lines), the PC-stable algorithm (red lines), and the MPC-stable algorithm (blue lines). Moreover, for each one of these algorithms we propose three different methods to estimate the CPDAGs and the causal effects: (1) use the original ordering of the variables (solid lines); (2) use the same methodology used in Stekhoven et al. (2012) with 100 stability selection runs but without permuting the variable orderings (labelled as + SS; dashed lines); and (3) use the same methodology used in Stekhoven et al. (2012) with 100 stability selection runs but permuting the variable orderings in each run (labelled as + SSP; dotted lines). The results are shown in Figure 12 where we investigate the performance for the top 20000 effects instead of the 5000 as in Figures 1(b) and 11.

We see that PC with stability selection and permuted variable orderings (PC + SSP) loses some performance at the beginning of the curve when compared to PC with standard

stability selection (PC + SS), but it has much better performance afterwards. The PC-stable algorithm with the original variable ordering performs very similar to PC plus stability selection (PC + SS) along the whole curve. Moreover, PC-stable plus stability selection (PC-stable + SS and PC-stable + SSP), loses a bit at the beginning of the curves but picks up much more signal later on in the curve. It is interesting to note that for PC-stable with stability selection, it makes little difference if the variable orderings are further permuted or not, even though PC-stable is not fully order-independent (see Figure 11). In fact, PC-stable plus stability selection (with or without permuted variable orderings) produces the best fit over all results.

7. Discussion

Due to their computational efficiency, constraint-based causal structure learning algorithms are often used in sparse high-dimensional settings. We have seen, however, that especially in these settings the order-dependence in these algorithms is highly problematic.

In this paper, we investigated this issue systematically, and resolved the various sources of order-dependence. There are of course many ways in which the order-dependence issues could be resolved, and we designed our modifications to be as simple as possible. Moreover, we made sure that existing high-dimensional consistency results for PC-, FCI- and RFCI-algorithms remain valid for their modifications under the same conditions. We showed that our proposed modifications yield improved and more stable estimation in sparse high-dimensional settings for simulated data, while their performances are similar to the performances of the original algorithms in low-dimensional settings.

Additionally to the order-dependence discussed in this paper, there is another minor type of order-dependence in the sense that the output of these algorithms also depends on the order in which the final orientation rules for the edges are applied. The reason is that an edge(mark) could be eligible for orientation by several orientation rules, and might be oriented differently depending on which rule is applied first. In our analyses, we have always used the original orderings in which the rules were given.

Compared to the adaptation of Cano et al. (2008), the modifications we propose are much simpler and we made sure that they preserve existing soundness, completeness, and high-dimensional consistency results. Finally, our modifications can be easily used together with other adaptations of constraint-based algorithms, for example hybrid versions of PC with score-based methods (Singh and Valtorta, 1993; Spirtes and Meek, 1995; van Dijk et al., 2003) or the PC* algorithm (Spirtes et al., 2000, Section 5.4.2.3).

All software is implemented in the R-package `pcalg` (Kalisch et al., 2012).

Acknowledgments

This research was supported in part by Swiss NSF grant 200021-129972. We thank Richard Fox, Markus Kalisch and Thomas Richardson for their valuable comments.

Appendix A. Additional Simulation Results

We now present additional simulation results for low-dimensional settings (Appendix A.1), high-dimensional settings (Appendix A.2) and medium-dimensional settings (Appendix A.3).

A.1 Estimation Performance in Low-Dimensional Settings

We considered the estimation performance in low-dimensional settings with less sparse graphs.

For the scenario without latent variables, we generated 250 random weighted DAGs with $p = 50$ and $E(N) = \{2, 4\}$, as described in Section 5.1. For each weighted DAG we generated an i.i.d. sample of size $n = 1000$. We then estimated each graph for 50 random orderings of the variables, using the sample versions of (L)PC(-stable), (L)CPC(-stable), and (L)MPC(-stable) with tuning parameter $\alpha \in \{0.000625, 0.00125, 0.0025, 0.005, 0.01, 0.02, 0.04\}$ for $E(N) = 2$ and $\alpha \in \{0.005, 0.01, 0.02, 0.04, 0.08, 0.16, 0.32\}$ for $E(N) = 4$ for the partial correlation tests. Thus, for each randomly generated graph, we obtained 50 estimated CPDAGs from each algorithm, for each value of α . Figure 13 shows the estimation performance of PC (circle; black line) and PC-stable (triangles; red line) for the skeleton. Figure 14 shows the estimation performance of all modifications of PC and PC-stable with respect to the CPDAGs in terms of SHD, and in terms of the variance of the SHD over the 50 random variable orderings per graph.

For the scenario with latent variables, we generated 120 random weighted DAGs with $p = 50$ and $E(N) = 2$, as described in Section 5.1. For each DAG we generated an i.i.d. sample size of $n = 1000$. To assess the impact of latent variables, we randomly defined in each DAG half of the variables that have no parents and at least two children to be latent. We then estimated each graph for 20 random orderings of the observed variables, using the sample versions of FCI(-stable), CFCI(-stable), MFCI(-stable), RFCI(-stable), CRFCI(-stable), and MRFCI(-stable) with tuning parameter $\alpha \in \{0.0025, 0.005, 0.01, 0.02, 0.04, 0.08\}$ for the partial correlation tests. Thus, for each randomly generated graph, we obtained 20 estimated PAGs from each algorithm, for each value of α . Figure 15 shows the estimation performance of FCI (circles; black dashed line), FCI-stable (triangles; red dashed line), RFCI (circles; black solid line), and RFCI-stable (triangles; red solid line) for the skeleton. Figure 16 shows the estimation performance for the PAGs in terms of SHD edge marks, and in terms of the variance of the SHD edge marks over the 20 random variable orderings per graph.

Regarding the skeletons of the CPDAGs and PAGs, the estimation performances between PC and PC-stable, as well as between (R)FCI and (R)FCI-stable are basically indistinguishable for all values of α . However, Figure 15 shows that FCI(-stable) returns graphs with slightly fewer edges than RFCI(-stable), for all values of α . This is related to the fact that FCI(-stable) tends to perform more tests than RFCI(-stable).

Regarding the CPDAGs and PAGs, the performance of the modifications of PC and (R)FCI (black lines) are very close to the performance of PC-stable and (R)FCI-stable (red lines). Moreover, CPC(-stable) and MPC(-stable) as well as C(R)FCI(-stable) and M(R)FCI(-stable) perform better in particular in reducing the variance of the SHD and SHD edge marks, respectively. This indicates that most of the order-dependence in the low-dimensional setting is in the orientation of the edges.

We also note that in all proposed measures there are only small differences between modifications of FCI and of RFCI.

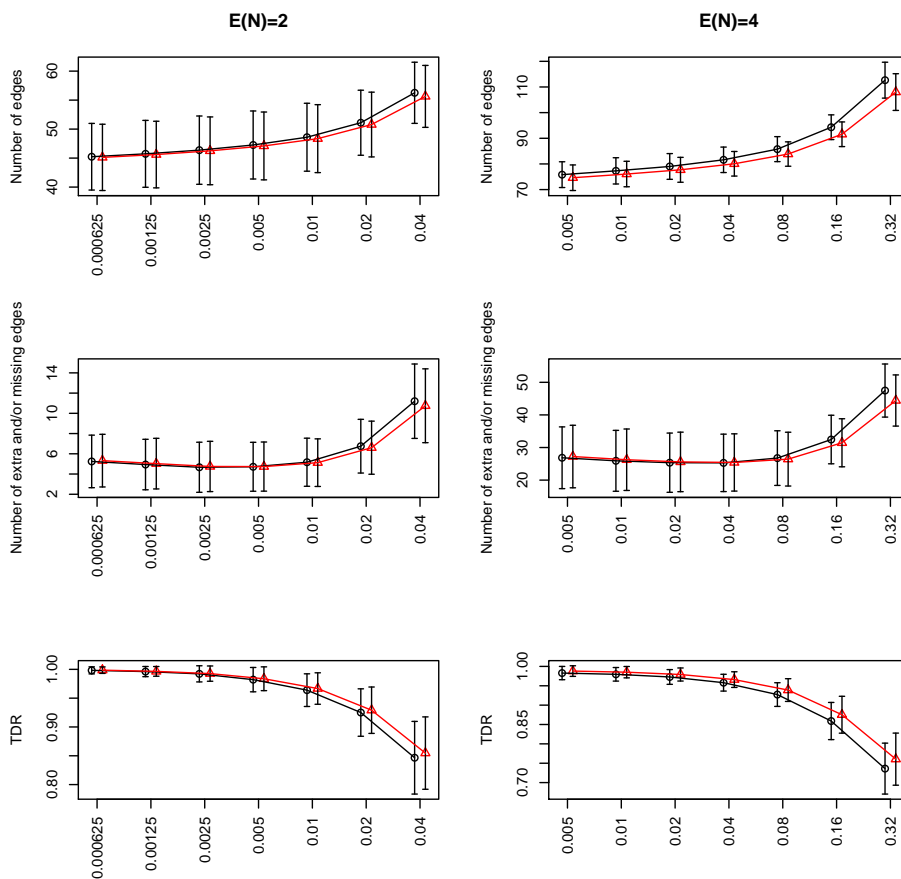


Figure 13: Estimation performance of PC (circles; black line) and PC-stable (triangles; red line) for the skeleton of the CPDAGs, for different values of α (x -axis displayed in log scale) in both low-dimensional settings. The results are shown as averages plus or minus one standard deviation, computed over 250 randomly generated graphs and 50 random variable orderings per graph, and slightly shifted up and down from the real values of α for a better visualization.

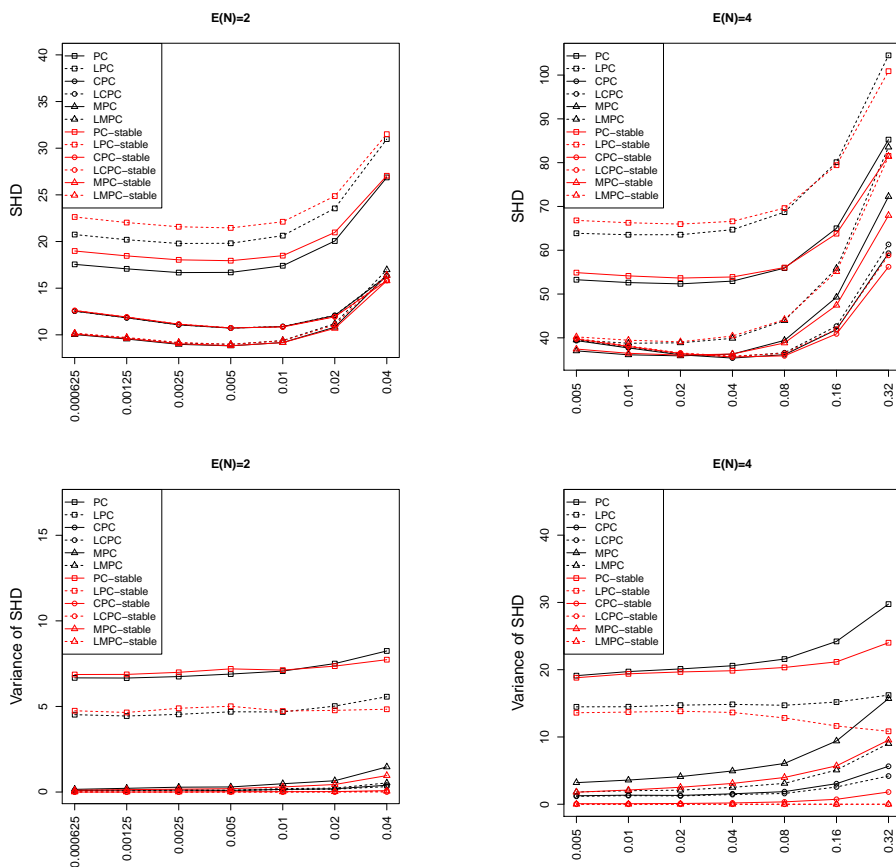


Figure 14: Estimation performance of (L)PC(-stable), (L)CPC(-stable), and (L)MPC(-stable) for the CPDAGs in the low-dimensional settings, for different values of α . The first row of plots shows the performance in terms of SHD, shown as averages over 250 randomly generated graphs and 50 random variable orderings per graph. The second row of plots shows the performance in terms of the variance of the SHD over the 50 random variable orderings per graph, shown as averages over 250 randomly generated graphs.

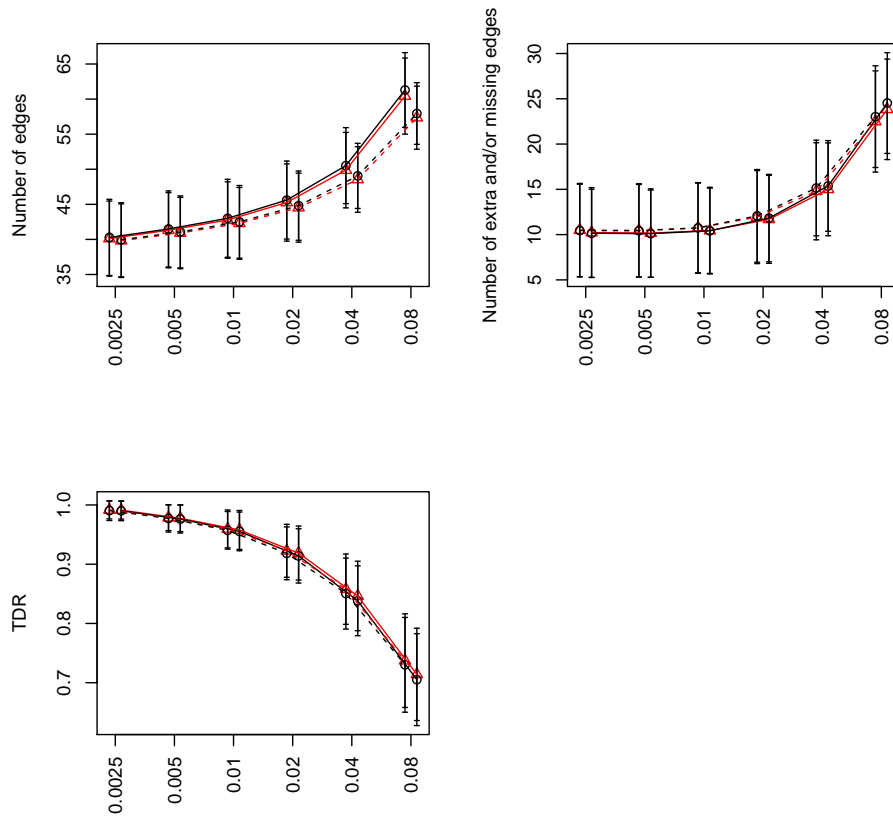


Figure 15: Estimation performance of FCI (circles; black dashed line), FCI-stable (triangles; red dashed line), RFCI (circles; black solid line), and RFCI-stable (triangles; red solid line), for the skeleton of the PAGs for different values of α (x -axis displayed in log scale) in the low-dimensional setting. The results are shown as averages plus or minus one standard deviation, computed over 120 randomly generated graphs and 20 random variable orderings per graph, and slightly shifted up and down from the real values of α for a better visualization.

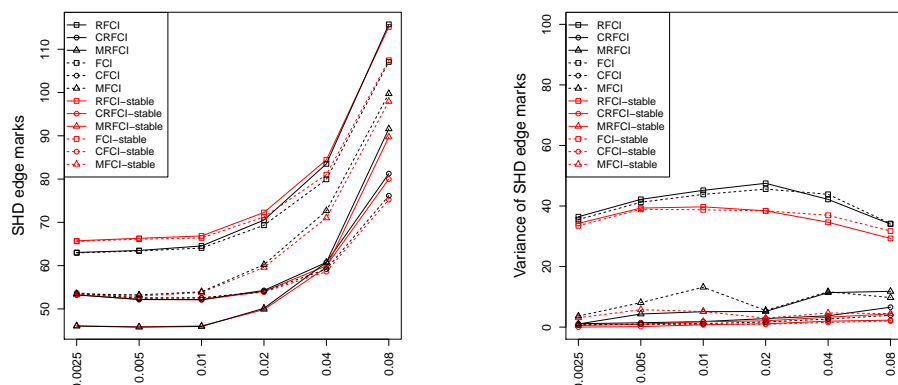


Figure 16: Estimation performance of the modifications of FCI(-stable) and RFCI(-stable) for the PAGs in the low-dimensional setting, for different values of α . The left panel shows the performance in terms of SHD edge marks, shown as averages over 120 randomly generated graphs and 20 random variable orderings per graph. The right panel shows the performance in terms of the variance of the SHD edge marks over the 20 random variable orderings per graph, shown as averages over 120 randomly generated graphs.

A.2 Number of Tests and Computing Time

We consider the number of tests and the computing time of PC and PC-stable in the high-dimensional setting described in Section 5.1.

One can easily deduce that Step 1 of the PC- and PC-stable algorithms perform the same number of tests for $\ell = 0$, because the adjacency sets do not play a role at this stage. Moreover, for $\ell = 1$ PC-stable performs at least as many tests as PC, since the adjacency sets $a(X_i)$ (see Algorithm 4.1) are always supersets of the adjacency sets $\text{adj}(X_i)$ (see Algorithm 3.2). For larger values of ℓ , however, it is difficult to analyze the number of tests analytically.

Table 4 therefore shows the average number of tests that were performed by Step 1 of the two algorithms, separated by size of the conditioning set, where we considered the high-dimensional setting with $\alpha = 0.04$ (see Section 5.2) since this was most computationally intensive. As expected the number of marginal correlation tests was identical for both algorithms. For $\ell = 1$, PC-stable performed slightly more than twice as many tests as PC, amounting to about 1.36×10^5 additional tests. For $\ell = 2$, PC-stable performed more tests than PC, amounting to 3.4×10^3 . For larger values of ℓ , PC-stable performed fewer tests than PC, since the additional tests for $\ell = 1$ and $\ell = 2$ lead to a sparser skeleton. However, since PC also performed relatively few tests for larger values of ℓ , the absolute difference in the number of tests for large ℓ is rather small. In total, PC-stable performed about 1.39×10^5 more tests than PC.

Table 5 shows the average runtime of the PC- and PC-stable algorithms. We see that PC-stable is somewhat slower than PC for all values of α , which can be explained by the fact that PC-stable tends to perform a larger number of tests (cf. Table 4).

	PC-algorithm	PC-stable algorithm
$\ell = 0$	5.21×10^5 (1.95×10^2)	5.21×10^5 (1.95×10^2)
$\ell = 1$	1.29×10^5 (2.19×10^3)	2.65×10^5 (4.68×10^3)
$\ell = 2$	1.10×10^4 (5.93×10^2)	1.44×10^4 (8.90×10^2)
$\ell = 3$	1.12×10^3 (1.21×10^2)	5.05×10^2 (8.54×10^1)
$\ell = 4$	9.38×10^1 (2.86×10^1)	3.08×10^1 (1.78×10^1)
$\ell = 5$	2.78×10^0 (4.53×10^0)	0.65×10^0 (1.94×10^0)
$\ell = 6$	0.02×10^0 (0.38×10^0)	-
Total	6.62×10^5 (2.78×10^3)	8.01×10^5 (5.47×10^3)

Table 4: Number of tests performed by Step 1 of the PC and PC-stable algorithms for each size of the conditioning sets ℓ , in the high-dimensional setting with $p = 1000$, $n = 50$ and $\alpha = 0.04$. The results are shown as averages (standard deviations) over 250 random graphs and 20 random variable orderings per graph.

	PC-algorithm	PC-stable algorithm	PC / PC-stable
$\alpha = 0.000625$	111.79 (7.54)	115.46 (7.47)	0.97
$\alpha = 0.00125$	110.13 (6.91)	113.77 (7.07)	0.97
$\alpha = 0.025$	115.90 (12.18)	119.67 (12.03)	0.97
$\alpha = 0.05$	116.14 (9.50)	119.91 (9.57)	0.97
$\alpha = 0.01$	121.02 (8.61)	125.81 (8.94)	0.96
$\alpha = 0.02$	131.42 (13.98)	139.54 (14.72)	0.94
$\alpha = 0.04$	148.72 (14.98)	170.49 (16.31)	0.87

Table 5: Run time in seconds (computed on an AMD Opteron(tm) Processor 6174 using R 2.15.1.) of PC and PC-stable for the high-dimensional setting with $p = 1000$ and $n = 50$. The results are shown as averages (standard deviations) over 250 random graphs and 20 random variable orderings per graph.

A.3 Estimation Performance in Settings where $p = n$

Finally, we consider two settings for the scenario with latent variables, where we generated 250 random weighted DAGs with $p = 50$ and $E(N) = \{2, 4\}$, as described in Section 5.1. For each DAG we generated an i.i.d. sample size of $n = 50$. We again randomly defined in each

DAG half of the variables that have no parents and at least two children to be latent. We then estimated each graph for 50 random orderings of the observed variables, using the sample versions of FCI(-stable), CFCI(-stable), MFCI(-stable), RFCI(-stable), CRFCI(-stable), and MRFCI(-stable) with tuning parameter $\alpha \in \{0.0025, 0.005, 0.01, 0.02, 0.04, 0.08, 0.16\}$ for $E(N) = 2$ and $\alpha \in \{0.005, 0.01, 0.02, 0.04, 0.08, 0.16, 0.32\}$ for $E(N) = 4$. Thus, for each randomly generated graph, we obtained 50 estimated PAGs from each algorithm, for each value of α .

Figure 17 shows the estimation performance for the skeleton. The (R)FCI-stable versions (red lines) lead to slightly sparser graphs and slightly better performance in TDR than (R)FCI versions (black lines) in both settings.

Figure 18 shows the estimation performance of all modifications of (R)FCI with respect to the PAGs in terms of SHD edge marks, and in terms of the variance of the SHD edge marks over the 50 random variable orderings per graph. The (R)FCI-stable versions produce a better fit than the (R)FCI versions. Moreover, C(R)FCI(-stable) and M(R)FCI(-stable) perform similarly for sparse graphs and they improve the fit, while in denser graphs M(R)FCI(-stable) still improves the fit and it performs much better than C(R)FCI(-stable) for the SHD edge marks. Again we see little difference between modifications of RFCI and FCI with respect to all measures.

Appendix B. Choice of the Tuning Parameter in the PC-Algorithm

We now discuss two possible methods for the choice of α in the PC-algorithm: one based on optimizing a Bayesian Information Criterion (BIC), and another based on stability selection.

In order to optimize the BIC, we take a grid of α 's. For each α , we compute the estimated CPDAG $\hat{G}(\alpha)$. Based on a DAG $\hat{G}'(\alpha)$ in the Markov equivalence class described $\hat{G}(\alpha)$, we then compute the maximum likelihood estimators $\hat{\Sigma}_{\hat{G}'(\alpha)}$ and $\hat{\mu}$ for the covariance matrix and mean vector of the Gaussian distribution of our variables X_1, \dots, X_p (Marchetti et al., 2012). Finally, we choose α to minimize

$$-2\ell\left(\hat{\Sigma}_{\hat{G}'(\alpha)}, \hat{\mu}\right) + \log n \left(\sum_{i \leq j} 1_{(\hat{\Sigma}_{\hat{G}'(\alpha)})_{ij} \neq 0} + p \right),$$

where $\ell(\cdot)$ denotes the log-likelihood of a p -dimensional multivariate Gaussian distribution. We point out, however, that one carefully needs to consider the behavior of BIC in the high-dimensional setting.

Another approach to tune the PC-algorithm is based on stability selection (Meinshausen and Bühlmann, 2010), which we also used in Section 6 (with permutations of the variable orderings) to solve order-dependence issues. For a rather large α , or for a range of α 's, one can investigate which edges are stable under a subsampling procedure, where stability is measured in terms of the relative frequency of occurrence of (directed or undirected) edges under the sub-sampling scheme. An edge is kept if it is stable, i.e., if the corresponding subsampling frequency is larger than a certain cut-off. One can also apply a stability selection procedure to IDA, where one considers the stability of the ranking of causal effects. The latter approach was taken in Stekhoven et al. (2012).

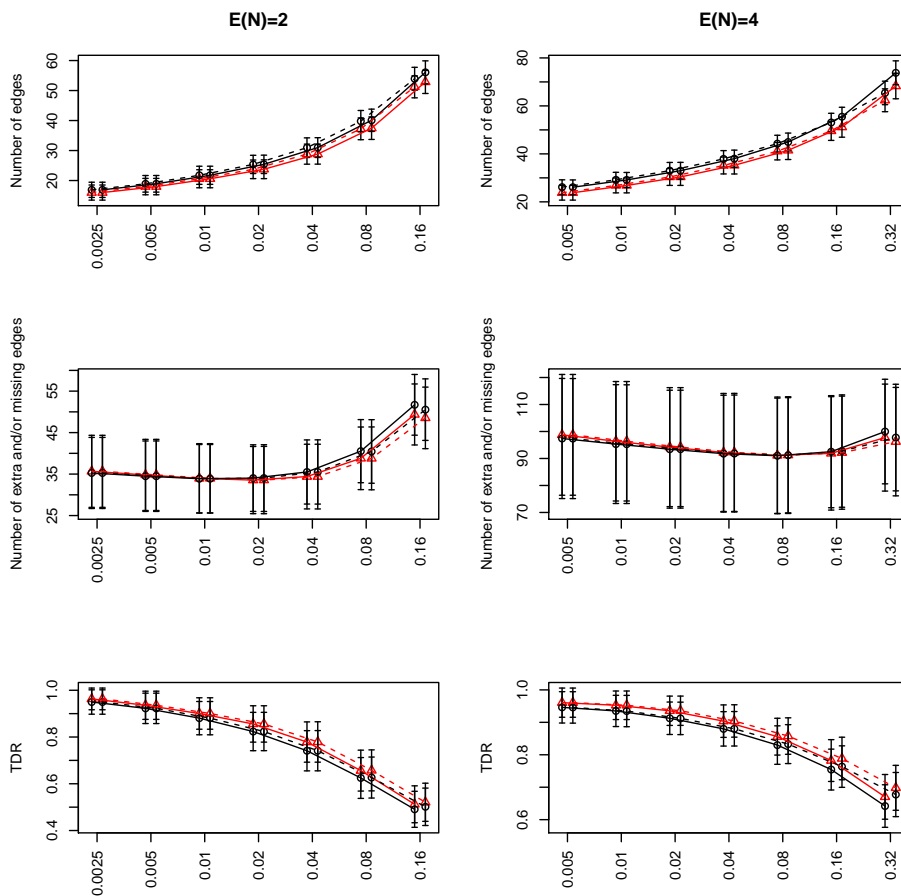


Figure 17: Estimation performance of FCI (circles; black dashed line), FCI-stable (triangles; red dashed line), RFCI (circles; black solid line), and RFCI-stable (triangles; red solid line), for the skeleton of the PAGs for different values of α (x -axis displayed in log scale) in two settings where $p = n$. The results are shown as averages plus or minus one standard deviation, computed over 250 randomly generated graphs and 50 random variable orderings per graph, and slightly shifted up and down from the real values of α for a better visualization.

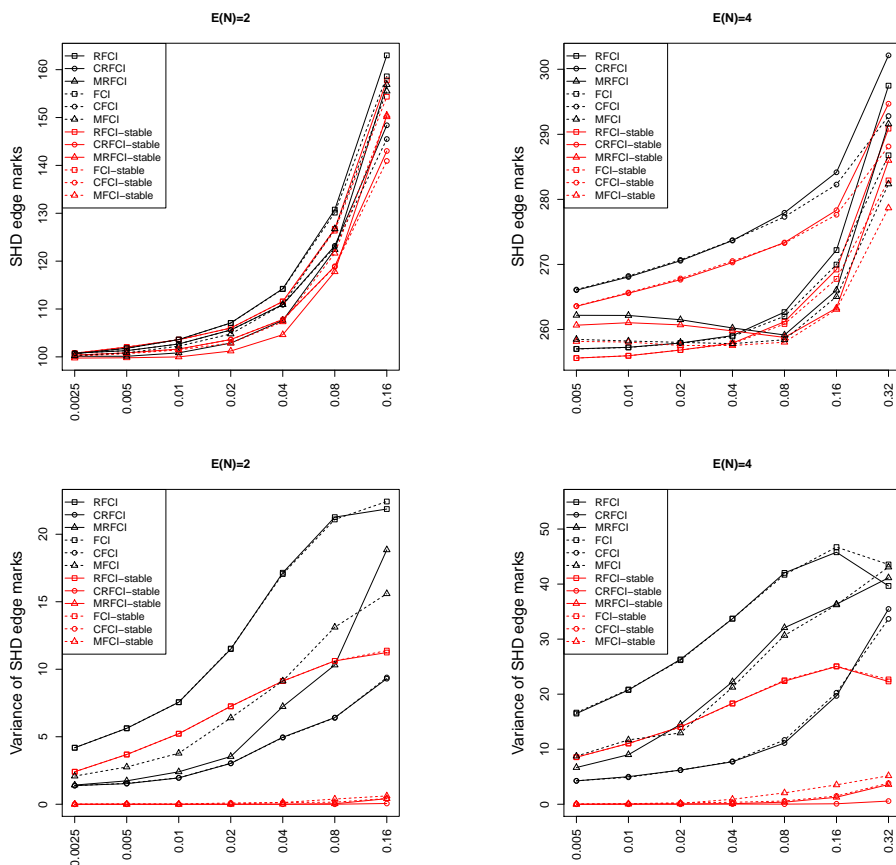


Figure 18: Estimation performance of the modifications of FCI(-stable) and RFCI(-stable) for the PAGs in settings where $p = n$, for different values of α . The first row of plots shows the performance in terms of SHD edge marks, shown as averages over 250 randomly generated graphs and 50 random variable orderings per graph. The second row of plots shows the performance in terms of the variance of the SHD edge marks over the 50 random variable orderings per graph, shown as averages over 250 randomly generated graphs.

References

- R.A. Ali, T.S. Richardson, and P. Spirtes. Markov equivalence for ancestral graphs. *Ann. Statist.*, 37:2808–2837, 2009.
- S. A. Andersson, D. Madigan, and M. D. Perlman. A characterization of Markov equivalence classes for acyclic digraphs. *Ann. Statist.*, 25:505–541, 1997.
- A. Cano, M. Gómez-Olmedo, and S. Moral. A score based ranking of the edges for the PC algorithm. In *Proceedings of the Fourth European Workshop on Probabilistic Graphical Models (PGM 2008)*, pages 41–48, 2008. Available at http://pgm08.cs.aau.dk/online_proc.html.
- D.M. Chickering. Learning equivalence classes of Bayesian-network structures. *J. Mach. Learn. Res.*, 2:445–498, 2002.
- T. Claassen, J. Mooij, and T. Heskes. Learning sparse causal models is not NP-hard. In *Proceedings of the 29th Conference on Uncertainty in Artificial Intelligence (UAI-2013)*, pages 172–181. AUAI Press, Corvallis, 2013.
- D. Colombo, M.H. Maathuis, M. Kalisch, and T.S. Richardson. Learning high-dimensional directed acyclic graphs with latent and selection variables. *Ann. Statist.*, 40:294–321, 2012.
- D. Dash and M.J. Druzdzel. A hybrid anytime algorithm for the construction of causal models from sparse data. In *Proceedings of the Fifteenth Conference on Uncertainty on Artificial Intelligence (UAI-1999)*, pages 142–149. Morgan Kaufmann, San Francisco, 1999.
- A.P. Dawid. Conditional independence for statistical operations. *Ann. Statist.*, 8:598–617, 1980.
- N. Harris and M. Drton. PC algorithm for nonparanormal graphical models. *J. Mach. Learn. Res.*, 14:3365–3383, 2013.
- T.R. Hughes, M.J. Marton, A.R. Jones, C.J. Roberts, R. Stoughton, C.D. Armour, H.A. Bennett, E. Coffey, H. Dai, Y.D. He, et al. Functional discovery via a compendium of expression profiles. *Cell*, 102:109–126, 2000.
- M. Kalisch and P. Bühlmann. Estimating high-dimensional directed acyclic graphs with the PC-algorithm. *J. Mach. Learn. Res.*, 8:613–636, 2007.
- M. Kalisch, B.A.G. Fellinghauer, E. Grill, M.H. Maathuis, U. Mansmann, P. Bühlmann, and G. Stucki. Understanding human functioning using graphical models. *BMC Med. Res. Methodol.*, 10(14), 2010.
- M. Kalisch, M. Mächler, D. Colombo, M.H. Maathuis, and P. Bühlmann. Causal inference using graphical models with the R package pcalg. *J. Stat. Softw.*, 47(11), 2012.
- M.H. Maathuis, M. Kalisch, and P. Bühlmann. Estimating high-dimensional intervention effects from observational data. *Ann. Statist.*, 37:3133–3164, 2009.

- M.H. Maathuis, D. Colombo, M. Kalisch, and P. Bühlmann. Predicting causal effects in large-scale systems from observational data. *Nature Methods*, 7:247–248, 2010.
- G.M. Marchetti, M. Drton, and K. Sadeghi. R-package `ggm`: Graphical Gaussian Models. Available at <http://cran.r-project.org>, 2012.
- C. Meek. Causal inference and causal explanation with background knowledge. In *Proceedings of the Eleventh Conference on Uncertainty in Artificial Intelligence (UAI-1995)*, pages 403–411. Morgan Kaufmann, San Francisco, 1995.
- N. Meinshausen and P. Bühlmann. Stability selection. *J. R. Stat. Soc. Series B*, 72:417–473, 2010.
- R. Nagarajan, S. Datta, M. Scutari, M. Beggs, G. Nolen, and C. Peterson. Functional relationships between genes associated with differentiation potential of aged myogenic progenitors. *Front. Physiol.*, 1(21), 2010.
- J. Pearl. *Causality: Models, reasoning, and inference*. Cambridge University Press, Cambridge, 2000.
- J. Pearl. Causal inference in statistics: An overview. *Statistics Surveys*, 3:96–146, 2009.
- J. Ramsey, J. Zhang, and P. Spirtes. Adjacency-faithfulness and conservative causal inference. In *Proceedings of the 22nd Annual Conference on Uncertainty in Artificial Intelligence (UAI-2006)*. AUAI Press, Arlington, 2006.
- T.S. Richardson. A discovery algorithm for directed cyclic graphs. In *Proceedings of the 12th Annual Conference on Uncertainty in Artificial Intelligence (UAI-1996)*, pages 454–461. Morgan Kaufmann, San Francisco, 1996.
- T.S. Richardson and P. Spirtes. Ancestral graph Markov models. *Ann. Statist.*, 30:962–1030, 2002.
- M. Singh and M. Valtorta. An algorithm for the construction of Bayesian network structures from data. In *Proceedings of the 9th Annual Conference on Uncertainty in Artificial Intelligence (UAI-1993)*, pages 259–265. Morgan Kaufmann, San Francisco, 1993.
- P. Spirtes. An anytime algorithm for causal inference. In *Proceedings of the 8th International Workshop on Artificial Intelligence and Statistics*, pages 213–221. Morgan Kaufmann, San Francisco, 2001.
- P. Spirtes and C. Meek. Learning Bayesian networks with discrete variables from data. In *Proceeding of the First International Conference on Knowledge Discovery and Data Mining (KDD-1995)*, pages 294–299, AAAI, Menlo Park, 1995.
- P. Spirtes, C. Glymour, and R. Scheines. *Causation, prediction, and search*. Springer-Verlag, New York, 1993.
- P. Spirtes, C. Meek, and T.S. Richardson. An algorithm for causal inference in the presence of latent variables and selection bias. In C. Glymour and G.F. Cooper, editors, *Computation, Causation and Discovery*, pages 211–252. MIT Press, Cambridge, 1999.

- P. Spirtes, C. Glymour, and R. Scheines. *Causation, Prediction, and Search*. MIT Press, Cambridge, second edition, 2000. With additional material by David Heckerman, Christopher Meek, Gregory F. Cooper and Thomas Richardson.
- D.J. Stekhoven, I. Moraes, G. Sveinbjörnsson, L. Hennig, M.H. Maathuis, and P. Bühlmann. Causal stability ranking. *Bioinformatics*, 28:2819–2823, 2012.
- S. van Dijk, L.C. van der Gaag, and D. Thierens. A skeleton-based approach to learning Bayesian networks from data. In *Proceedings of the 7th Conference on Principles and Practice of Knowledge Discovery in Databases (PKDD-2003)*, pages 132–143. Springer, Berlin, 2003.
- J. Zhang. On the completeness of orientation rules for causal discovery in the presence of latent confounders and selection bias. *Artif. Intell.*, 172:1873–1896, 2008.
- X. Zhang, X.M. Zhao, K. He, L. Lu, Y. Cao, J. Liu, J.K. Hao, Z.P. Liu, and L. Chen. Inferring gene regulatory networks from gene expression data by path consistency algorithm based on conditional mutual information. *Bioinformatics*, 28:98–104, 2012.